

Analysis of the b_1 meson decay in local tensor bilinear representation

Kie Sang Jeong^a Su Houg Lee^b Yongseok Oh^{c,a}

^a*Asia Pacific Center for Theoretical Physics, Pohang, Gyeongbuk 37673, Korea*

^b*Department of Physics and Institute of Physics and Applied Physics, Yonsei University, Seoul 03722, Korea*

^c*Department of Physics, Kyungpook National University, Daegu 41566, Korea*

E-mail: kiesang.jeong@apctp.org, suhoug@yonsei.ac.kr, yohphy@knu.ac.kr

ABSTRACT: We explore the validity of vector meson dominance in the radiative decay of the $b_1(1235)$ meson. In order to explain the violation of the vector meson dominance hypothesis in this decay process, we investigate a model where the b_1 meson strongly couples with the local current in tensor bilinear representation. The tensor representation is investigated in the framework of the operator product expansion and we found a low energy decay process that does not follow the usual vector meson dominance hypothesis. The ω -like intermediate meson state of quantum numbers $I^G(J^{PC}) = 0^-(1^{--})$ is found to have a nontrivial role in the decay process of the b_1 meson. The spectral structure of the ω -like state is found to be close to a π - ρ hybrid state, which provides a mechanism that evades the usual vector meson dominance hypothesis. Precise measurements of various decay channels of the b_1 meson are, therefore, required to unravel the internal structure of axial vector mesons.

Contents

1	Introduction	1
2	Phenomenology of the b_1 meson	3
2.1	Strong decay	3
2.2	Radiative decay and vector meson dominance	5
3	Spin-1 mesons in local tensor bilinear representation	6
3.1	Brief review on local bilinear representation of spin-1 mesonic state	6
3.2	b_1 meson decay in the soft pion limit	8
4	Operator product expansion and spectral sum rules	10
4.1	OPE of the correlators	10
4.2	Spectral sum rules	11
5	Discussion and Conclusion	18
A	Tensor currents in $SU(2)_L \times SU(2)_R$ symmetry	20
A.1	Transformation of tensor currents in the non-relativistic limit	20
A.2	Transformation of tensor currents in relativistic generalization	21
B	Technical remarks on sum rules analysis	22
B.1	Four-quark condensates	22
B.2	Supplementary remarks for the sum rules with $\alpha_A < 0$, $\beta_A < 0$	24
B.3	Borel sum rules	25

1 Introduction

According to the Particle Data Group [1], the axial-vector $b_1(1235)$ meson has a mass of 1229.5 ± 3.2 MeV and quantum numbers $I^G(J^{PC}) = 1^+(1^{+-})$. Its decay width is estimated to be $\Gamma(b_1) = 142 \pm 9$ MeV, which is dominated by the $b_1 \rightarrow \pi\omega$ decay channel. In particular, the D -wave to S -wave amplitude ratio in the decay of $b_1 \rightarrow \pi\omega$ is found to be $D/S = 0.277 \pm 0.027$.¹ The radiative decays of the $b_1(1235)$ meson were also observed and the width is estimated as $\Gamma(b_1 \rightarrow \pi^\pm\gamma) = 230 \pm 60$ keV [1, 3].² Since most strong decays of the b_1 meson is in the $\pi\omega$ channel, its radiative decay into $\pi\gamma$ can be another test for the vector meson dominance (VMD) hypothesis.

¹The $b_1 \rightarrow \pi\rho$ decay violates G -parity conservation. The most recent measurement performed at the Brookhaven National Laboratory gives $D/S = 0.269 \pm (0.009)_{\text{stat}} \pm (0.01)_{\text{sys}}$ [2].

²The radiative decay of $b_1 \rightarrow \pi^0\gamma$ is yet to be measured.

If the U(1) symmetry part of the vector meson field is conserved, the vector meson field plays the role of the external electromagnetic field source through the direct coupling in the form of $\mathcal{L}_{\gamma\omega} \sim A_\mu V^\mu$ [4–8]. This argument is based on the assumption that the vector meson has the same representation as the electromagnetic current.³ According to the VMD hypothesis, it is natural to assume that the radiative b_1 decay is dominated by the intermediate ω meson, namely, it leads to the decay chain of $b_1 \rightarrow \pi^\pm \omega \rightarrow \pi^\pm \gamma$. However, as will be discussed in Sec. 2, such VMD model underestimates the decay width of $b_1 \rightarrow \pi^\pm \gamma$ [13, 14], and this may imply the possibility that there might be a missing source or mechanism for the radiative decays of the b_1 meson, which dominates over the mechanism proposed by the VMD hypothesis. The present work is motivated by the idea that, if the intermediate spin-1 mesonic state is not in exactly the same representation with the electromagnetic current, then there could be an additional process for the b_1 radiative decay that cannot be ascribed to the VMD hypothesis alone. In other words, another representation for spin-1 mesonic states can be allowed if it overlaps with the U(1) gauge boson in low energy regime where flavor symmetry is broken down to $SU(2)_V$ [15, 16]. In this case, the state with the quantum numbers of the ω meson, usually represented by chiral vector current, can also be represented in the helicity mixed space via a tensor current. We denote this state as $\bar{\omega}$. In this helicity mixed representation, the $b_1 \rightarrow \pi \bar{\omega}$ decay can be regarded as a production process of a soft-pion as the b_1 and $\bar{\omega}$ states are chiral partners to each other.

In this study, the properties of the tensor representation for spin-1 mesonic current is reviewed and their current correlation function is calculated in the framework of operator product expansion (OPE) [17]. We first discuss the spin-1 mesonic state interpolated by tensor currents and the b_1 decay process in the context of chiral rotation [18, 19]. The distinct nature of the spin-1 mesonic state in the tensor current correlation is analyzed through QCD sum rules [20–25]. In the OPE of tensor current correlator, the four-quark condensates appear as the leading quark contribution. Although the vacuum saturation hypothesis for the four-quark condensate has been widely used in previous studies, it does not reflect all the possible vacuum structure of QCD. The factorization scheme is modified to take into account the non-factorizable part and quark correlation pattern in topologically nontrivial gauge configuration [26–32]. Within the usual limit of the factorization parameters, we will show that the tensor current can strongly couple to the b_1 meson as well as to the π - ρ continuum state that has the quantum numbers of the ω meson. Analyzing the $b_1 \rightarrow \pi \bar{\omega}$ decay within the soft pion limit, we find that the ω -like mesonic state $\bar{\omega}$, which appears in the strong decay of the b_1 into the pion, would not be a simple one-particle state but an anomalous hybrid state. Our analyses will show that this process would be a source for b_1 radiative decays instead of the usual VMD mechanism.

This paper is organized as follows. In section 2, we discuss the problems in the phenomenology of the b_1 meson decays. In section 3, a brief review on local bilinear representations of spin-1 mesonic state and their evolution in chiral symmetry breaking is presented. Detailed OPE for correlation functions and corresponding spectral analyses with four-quark

³The realization of VMD in effective Lagrangian approaches can be found, for example, in Refs. [9–12].

condensates are presented in section 4. Section 5 contains discussion and conclusions. We leave the details on tensor currents and technical remarks on sum rule analysis in Appendixes.

2 Phenomenology of the b_1 meson

In this Section, we review the phenomenology of the b_1 meson decays. The major strong decay channel, i.e., $b_1 \rightarrow \pi\omega$, is discussed and then its radiative decays is discussed in connection with the VMD hypothesis.

2.1 Strong decay

In quark models, the $b_1(1235)$ state is described as a member of the 1P_1 nonet (in the ${}^{2S+1}L_J$ notation), where the $q\bar{q}$ pair is in the relative P -wave state, having quantum numbers $J^{PC} = 1^{+-}$. Other members of this nonet may include the $h_1(1170)$ and $h_1(1380)$ which are iso-scalars, and $K_1(1270)$ or $K_1(1400)$ that has one unit of strangeness [14].

The strong decay of the b_1 meson is described by the amplitude of an axial-vector meson ($J^P = 1^+$) decay into a vector meson ($J^P = 1^-$) plus a pseudoscalar meson ($J^P = 0^-$), which reads

$$\mathcal{M}(1^+ \rightarrow 1^- 0^-) = \varepsilon_\nu^*(1^-, p_V) \Gamma^{\mu\nu}(1^+ \rightarrow 1^- 0^-) \varepsilon_\mu(1^+, p_A), \quad (2.1)$$

where $\varepsilon_\mu(1^\pm, p)$ represents the polarization vector of $J^P = 1^\pm$ meson with momentum p . Here, p_A and p_V are the momenta of the axial-vector meson and the vector meson, respectively, and the momentum of the pseudoscalar meson p_P is determined by the energy-momentum conservation, $p_A = p_V + p_P$. The most general form of the amplitude $\Gamma^{\mu\nu}$ reads [33]

$$\begin{aligned} \Gamma^{\mu\nu}(1^+ \rightarrow 1^- 0^-) = & f_1 g^{\mu\nu} + f_2 (p_V - p_P)^\mu (p_A + p_P)^\nu + f_3 (p_V + p_P)^\mu (p_A + p_P)^\nu \\ & + f_4 (p_V - p_P)^\mu (p_A - p_P)^\nu + f_5 (p_V + p_P)^\mu (p_A - p_P)^\nu, \end{aligned} \quad (2.2)$$

where f_i 's are form factors. If all of the particles in the decay process are on-mass shell, only the two terms, f_1 and f_2 , are non-vanishing because of $\varepsilon(1^-, p_V) \cdot p_V = \varepsilon(1^+, p_A) \cdot p_A = 0$.

Therefore, the decay amplitude for $b_1 \rightarrow \pi\omega$ constrained by gauge invariance reads [33]

$$\langle \omega(k) \pi | H_{\text{int}} | b_1(q) \rangle = -i \varepsilon_\nu^*(\omega, k) \Gamma^{\mu\nu} \varepsilon_\mu(b_1, q), \quad (2.3)$$

where the momenta of the b_1 and ω mesons are represented by q and k , respectively, and

$$\begin{aligned} \Gamma^{\mu\nu} = & F_{b_1\omega\pi} \left(g^{\mu\nu} - \frac{k^\mu k^\nu}{k^2} - \frac{q^\mu q^\nu}{q^2} + \frac{k \cdot q}{k^2 q^2} q^\mu k^\nu \right) \\ & + G_{b_1\omega\pi} \left(k^\mu - \frac{k \cdot q}{q^2} q^\mu \right) \left(q^\nu - \frac{k \cdot q}{k^2} k^\nu \right). \end{aligned} \quad (2.4)$$

Because of the transversality condition, $\varepsilon(p) \cdot p = 0$, however, the terms with q^μ or k^ν vanish, and we can rewrite it effectively as

$$\Gamma^{\mu\nu} = F_{b_1\omega\pi} g^{\mu\nu} + G_{b_1\omega\pi} k^\mu q^\nu. \quad (2.5)$$

By introducing dimensionless form factors, f and h , we can write [34]

$$\Gamma^{\mu\nu} = M_{b_1} \left[fg^{\mu\nu} + \frac{h}{M_\omega M_{b_1}} q^\nu k^\mu \right], \quad (2.6)$$

where M_{b_1} and M_ω are the masses of the b_1 meson and ω meson, respectively. Then the decay width is calculated as

$$\Gamma(b_1 \rightarrow \omega\pi) = \frac{|\mathbf{k}|}{24\pi} \left\{ 2f^2 + \frac{1}{M_\omega^4} (E_\omega M_\omega f + |\mathbf{k}|^2 h)^2 \right\}, \quad (2.7)$$

where E_ω is the energy of the ω meson, $E_\omega = \sqrt{M_\omega^2 + |\mathbf{k}|^2}$. Also from the definitions of the S - and D -wave amplitudes,

$$\begin{aligned} \langle \omega(\mathbf{k}, m_\omega) \pi(-\mathbf{k}) | H_{\text{int}} | b_1(\mathbf{0}, m_b) \rangle &= if^S \delta_{m_\omega m_b} Y_{00}(\Omega_k) \\ &+ if^D \sum_{m_\ell} \langle 2m_\ell 1m_\omega | 1m_b \rangle Y_{2m_\ell}(\Omega_k), \end{aligned} \quad (2.8)$$

we have

$$\begin{aligned} f^S &= \frac{\sqrt{4\pi} M_{b_1}}{3M_\omega^2} [M_\omega(E_\omega + 2M_\omega)f + |\mathbf{k}|^2 h], \\ f^D &= -\frac{\sqrt{8\pi} M_{b_1}}{3M_\omega^2} [M_\omega(E_\omega - M_\omega)f + |\mathbf{k}|^2 h], \end{aligned} \quad (2.9)$$

which gives

$$R = f^D/f^S = -\frac{\sqrt{2} \{M_\omega(E_\omega - M_\omega)f + |\mathbf{k}|^2 h\}}{\{M_\omega(E_\omega + 2M_\omega)f + |\mathbf{k}|^2 h\}}. \quad (2.10)$$

The magnitude of the momentum \mathbf{k} is

$$|\mathbf{k}| = \frac{1}{2M_{b_1}} \sqrt{\lambda(M_{b_1}^2, M_\omega^2, M_\pi^2)}, \quad (2.11)$$

where $\lambda(x, y, z) = x^2 + y^2 + z^2 - 2xy - 2yz - 2zx$ is the Källén function. This gives $|\mathbf{k}| = 346.5$ MeV with $M_{b_1} = 1.230$ GeV, $M_\omega = 0.783$ MeV, and $M_\pi = 0.140$ GeV. From the two experimental data,

$$\Gamma(b_1 \rightarrow \omega\pi) \simeq \Gamma(b_1) = 142 \pm 9 \text{ MeV}, \quad f^D/f^S = 0.277 \pm 0.027, \quad (2.12)$$

we obtain

$$f = 3.70, \quad h = -11.04, \quad (2.13)$$

up to the overall phase, which leads to⁴

$$h/f = -2.98. \quad (2.14)$$

⁴Note that this is very different from the old estimation of Refs. [35–37], which obtained $h/f \approx +9.0$ by fitting the high energy data of $\pi N \rightarrow \omega N$ with the exchanges of the b_1 and ρ trajectories.

One can relate the above information with the couplings of the effective $b_1\omega\pi$ interaction Lagrangian,

$$\mathcal{L} = g_1 M_{b_1} \omega_\mu \mathbf{b}_1^\mu \cdot \boldsymbol{\pi} + \frac{g_2}{M_{b_1}} \omega_{\mu\nu} \mathbf{b}_1^{\mu\nu} \cdot \boldsymbol{\pi}, \quad (2.15)$$

where ω^μ and b_1^μ are the ω meson field and the b_1 meson field, respectively, and their field strength tensors are

$$\omega_{\mu\nu} = \partial_\mu \omega_\nu - \partial_\nu \omega_\mu, \quad b_1^{\mu\nu} = \partial^\mu b_1^\nu - \partial^\nu b_1^\mu, \quad (2.16)$$

and $\mathbf{b}_1^\mu \cdot \boldsymbol{\pi} = b_1^0 \pi^0 + b_1^+ \pi^- + b_1^- \pi^+$.⁵ The above Lagrangian gives

$$\Gamma^{\mu\nu}(b_1 \rightarrow \omega\pi) = (g_1 + 2g_2 k \cdot q) g^{\mu\nu} - 2g_2 k^\mu q^\nu. \quad (2.17)$$

Comparing with Eq. (2.5) we have

$$\begin{aligned} F_{b\omega\pi} &= M_{b_1} f = M_{b_1} g_1 + \frac{2k \cdot q}{M_{b_1}} g_2, \\ G_{b\omega\pi} &= \frac{h}{M_\omega} = -\frac{2}{M_{b_1}} g_2. \end{aligned} \quad (2.18)$$

Then we can estimate the coupling constants as

$$g_1 = -1.34 \quad g_2 = 8.61. \quad (2.19)$$

2.2 Radiative decay and vector meson dominance

The radiative decay of $b_1 \rightarrow \pi\gamma$ was investigated in quark models based on the VMD hypothesis. The VMD hypothesis leads to

$$\Gamma(b_1 \rightarrow \gamma\pi) = \left(\frac{|\mathbf{p}_\gamma|}{|\mathbf{p}_\pi|} \right)^n \frac{\alpha_{\text{em}}}{g_\omega^2/4\pi} \Gamma(b_1 \rightarrow \omega_\perp \pi), \quad (2.20)$$

where ω_\perp represents the transverse component of the ω vector meson and g_ω is the coupling of the ω meson to the photon in VMD that is estimated as $g_\omega \approx 17.14$. The magnitudes of the momenta of the decays are $|\mathbf{p}_\gamma| = 607.0$ MeV and $|\mathbf{p}_\pi| = 346.5$ MeV. Here, n shows the characteristic momentum dependence of the decay process, of which values will be discussed later.

The decay amplitude of the strong decay of the b_1 into the transverse ω meson can be estimated following Ref. [13]. The transverse and longitudinal decay amplitudes of the $b_1 \rightarrow \omega\pi$ decay are related to the S and D wave amplitudes as

$$A_1 = f^S + \frac{1}{\sqrt{2}} f^D, \quad A_0 = f^S - \sqrt{2} f^D, \quad (2.21)$$

which gives

$$A_1 = \sqrt{4\pi} M_{b_1} f, \quad A_0 = \frac{\sqrt{4\pi} M_{b_1}}{M_\omega^2} (M_\omega E_\omega f + |\mathbf{k}|^2 h). \quad (2.22)$$

⁵This flavor structure is consistent with the form of $\text{Tr}(V[B, P]_+)$, which should be compared with the axial-vector meson interaction that comes from the structure of $\text{Tr}(V[A, P]_-)$. Here, V , A , B , P are the vector meson octet, axial-vector meson octet including the a_1 meson, axial-vector meson octet including the b_1 meson, and pseudoscalar meson octet and $[A, B]_\pm = AB \pm BA$.

So we have

$$\frac{\Gamma(b_1 \rightarrow \omega_\perp \pi)}{\Gamma(b_1 \rightarrow \omega \pi)} = \frac{2|A_1|^2}{2|A_1|^2 + |A_0|^2} = \frac{2 + 2\sqrt{2}R + R^2}{3(1 + R^2)} \simeq 0.8855, \quad (2.23)$$

where the experimental value $R \equiv f^D/f^S = 0.277$ is used. Then we have $\Gamma(b_1 \rightarrow \omega_\perp \pi) \approx 126$ MeV.

In Ref. [13], $n = 3$ is used in the expression of Eq. (2.20), which gives

$$\Gamma(b_1 \rightarrow \gamma \pi) \approx 210 \text{ keV}. \quad (2.24)$$

This seems to be successful to explain the observed value $\Gamma(b_1 \rightarrow \gamma \pi)_{\text{expt.}} = 230 \pm 60$ keV. However, it was pointed out in Ref. [14] that the VMD prediction is sensitive to the interaction form which determines the value of n . Using the covariant oscillator quark model, the authors of Ref. [14] predicted

$$\Gamma(b_1 \rightarrow \gamma \pi) \approx 69 \text{ keV}. \quad (2.25)$$

This is very similar to the value obtained with $n = 1$ in Eq. (2.20). However, the general form of the $b_1 \omega \pi$ interaction contains two terms as shown in Eq. (2.7). In fact, the expression for the decay width (2.7) contains terms with $n = 1, 3,$ and 5 . Following Ref. [13], we estimate the radiative decay width of b_1 by replacing \mathbf{k} by \mathbf{p}_γ and

$$f \rightarrow \frac{\sqrt{\alpha_{\text{em}}}}{g_\omega/\sqrt{4\pi}} f, \quad h \rightarrow \frac{\sqrt{\alpha_{\text{em}}}}{g_\omega/\sqrt{4\pi}} h \quad (2.26)$$

in the decay width formula of Eq. (2.7). Taking into account that $\Gamma(b_1 \rightarrow \omega_\perp \pi) \approx 126$ MeV, we obtain

$$\Gamma(b_1 \rightarrow \gamma \pi) \approx 160 \text{ keV}, \quad (2.27)$$

which is about 2/3 of the measured quantity.

3 Spin-1 mesons in local tensor bilinear representation

Throughout this study, the isospin flavor matrices are denoted as $T^0 = I/2$, $T^a = \sigma^a/2$, where I is the 2×2 unit matrix and σ^a is the Pauli matrix. These matrices are normalized as $\text{Tr}[T^A T^B] = \delta^{AB}/2$. Here, capital romans ($A = 0 - 3$) denote isospin ($0 \oplus 1$) indices and lower-case romans ($a = 1 - 3$) denote isovector indices. We will use barred romans ($\bar{a} = 1 - 8$) to denote adjoint color indices in gauge interactions. Mesonic quantum numbers are represented by $[I^G(J^{PC})]$.

3.1 Brief review on local bilinear representation of spin-1 mesonic state

The simplest local representation of the b_1 meson is $\bar{q} T^a \gamma_5 \overleftrightarrow{D}_\mu q$. This current is in helicity mixed representation $(\frac{1}{2}, \frac{1}{2}) \oplus (\frac{1}{2}, \frac{1}{2})$, where the first and second numbers in the bracket show the $\text{SU}(2)_L$ and $\text{SU}(2)_R$ representations, respectively. The derivative leads to additional p^2 factors in the Wilson coefficient of OPE terms, which makes the OPE dominated by the continuum contribution [23]. In the same representation, tensor current $\bar{q} T^a \sigma_{\mu\nu} q$, which

does not contain the covariant derivative, can also be considered. This current can couple to four different spin-1 mesonic systems. In the non-relativistic limit, where $p_\mu \rightarrow (m, \mathbf{0})$, depending on the intrinsic quantum numbers, the spin-1 mesonic states of momentum p and polarization λ have the following relations: [16]

$$\bar{\omega} : [I^G J^{PC} = 0^-(1^{--})] \rightarrow \langle 0 | \bar{q} T^0 \sigma_{0k} q | \bar{\omega}(p, \lambda) \rangle = i f_\omega^T (-\bar{\epsilon}_k^{(\lambda)} p_0), \quad (3.1)$$

$$\begin{aligned} \bar{h}_1 : [I^G J^{PC} = 0^-(1^{+-})] &\rightarrow \langle 0 | \bar{q} T^0 \sigma_{ij} q | \bar{h}_1(p, \lambda) \rangle = i f_{h_1}^T \epsilon_{ijk} (-\bar{\epsilon}_k^{(\lambda)} p_0) \\ &\rightarrow \frac{1}{2} \epsilon_{ijk} \langle 0 | \bar{q} T^0 \sigma_{ij} q | \bar{h}_1(p, \lambda) \rangle = i f_{h_1}^T (-\bar{\epsilon}_k^{(\lambda)} p_0), \end{aligned} \quad (3.2)$$

$$\bar{\rho} : [I^G J^{PC} = 1^+(1^{--})] \rightarrow \langle 0 | \bar{q} T^a \sigma_{0k} q | \bar{\rho}(p, \lambda) \rangle = i f_{\rho^a}^T (-\bar{\epsilon}_k^{(\lambda)} p_0), \quad (3.3)$$

$$\begin{aligned} \bar{b}_1 : [I^G J^{PC} = 1^+(1^{+-})] &\rightarrow \langle 0 | \bar{q} T^a \sigma_{ij} q | \bar{b}_1(p, \lambda) \rangle = i f_{b_1^a}^T \epsilon_{ijk} (-\bar{\epsilon}_k^{(\lambda)} p_0) \\ &\rightarrow \frac{1}{2} \epsilon_{ijk} \langle 0 | \bar{q} T^a \sigma_{ij} q | \bar{b}_1(p, \lambda) \rangle = i f_{b_1^a}^T (-\bar{\epsilon}_k^{(\lambda)} p_0), \end{aligned} \quad (3.4)$$

where the bar notation is used *to distinguish the mesonic states of the helicity mixed tensor current representation from those of chiral vector representation*.⁶ For example, the $\bar{\omega}$ is the state of tensor current representation having $I^G J^{PC} = 0^-(1^{--})$ as the usual ω meson. Here, $\bar{\epsilon}_\mu^{(\lambda)}$ is the polarization vector and the vector meson coupling is given by f_V^T in tensor representation. In a boosted frame, $p_\mu \rightarrow (\sqrt{m^2 + \mathbf{p}^2}, \mathbf{p})$, the covariant generalizations read

$$\bar{\omega} \rightarrow \langle 0 | \bar{q} T^0 \sigma_{\mu\nu} q | \bar{\omega}(p, \lambda) \rangle = i f_\omega^T (\bar{\epsilon}_\mu^{(\lambda)} p_\nu - \bar{\epsilon}_\nu^{(\lambda)} p_\mu), \quad (3.5)$$

$$\bar{h}_1 \rightarrow -\frac{1}{2} \epsilon_{\mu\nu\alpha\beta} \langle 0 | \bar{q} T^0 \sigma^{\alpha\beta} q | \bar{h}_1(p, \lambda) \rangle = i f_{h_1}^T (\bar{\epsilon}_\mu^{(\lambda)} p_\nu - \bar{\epsilon}_\nu^{(\lambda)} p_\mu), \quad (3.6)$$

$$\bar{\rho} \rightarrow \langle 0 | \bar{q} T^a \sigma_{\mu\nu} q | \bar{\rho}(p, \lambda) \rangle = i f_{\rho^a}^T (\bar{\epsilon}_\mu^{(\lambda)} p_\nu - \bar{\epsilon}_\nu^{(\lambda)} p_\mu), \quad (3.7)$$

$$\bar{b}_1 \rightarrow -\frac{1}{2} \epsilon_{\mu\nu\alpha\beta} \langle 0 | \bar{q} T^a \sigma^{\alpha\beta} q | \bar{b}_1(p, \lambda) \rangle = i f_{b_1^a}^T (\bar{\epsilon}_\mu^{(\lambda)} p_\nu - \bar{\epsilon}_\nu^{(\lambda)} p_\mu), \quad (3.8)$$

The tensor current couples only to the transverse polarization of spin-1 mesonic state [15, 24, 25] because of the relation,

$$\begin{aligned} \langle 0 | \bar{q} T^A \sigma_{\mu\nu} q | [1^{--}](p, \lambda) \rangle &= i f_{VA}^T \left\{ \bar{\epsilon}_\mu^{(\lambda)} p_\nu - \bar{\epsilon}_\nu^{(\lambda)} p_\mu \right\} \\ &= i f_{VA}^T \left\{ (g_{\mu\bar{\mu}} - p_\mu p_{\bar{\mu}}/p^2) \bar{\epsilon}^{(\lambda)\bar{\mu}} p_\nu - (g_{\nu\bar{\nu}} - p_\nu p_{\bar{\nu}}/p^2) \bar{\epsilon}^{(\lambda)\bar{\nu}} p_\mu \right\} \\ &= i f_{VA}^T \left\{ \bar{\epsilon}_\mu^{t(\lambda)} p_\nu - \bar{\epsilon}_\nu^{t(\lambda)} p_\mu \right\}, \end{aligned} \quad (3.9)$$

where $\bar{\epsilon}_\mu^{t(\lambda)}$ denotes the transverse polarization vector. However, this current couples to both the parity-even and parity-odd modes, and each parity mode can be separately projected

⁶If we extend this formalism to flavor SU(3), there should be states of open and hidden strangeness in tensor representation [16]. In the quark model, the $K_1(1270)$ and $K_1(1400)$ are interpreted as mixtures of 1P_1 and 3P_1 states [14]. Since the b_1 is a member of the 1P_1 multiplet in the quark model, both K_1 states may be mixed states of vector and tensor representations. More rigorous investigation is required to understand the SU(3) realization of tensor representation, but is beyond the scope of this work.

out from the current-current correlation as

$$\sum_{\lambda} \langle 0 | \bar{q} T^A \sigma_{\mu\bar{\mu}} q | [1^{--}](p, \lambda) \rangle \langle [1^{--}](p, \lambda) | \bar{q} T^B \sigma_{\nu\bar{\nu}} q | 0 \rangle = -\delta^{AB} (f_-^T)^2 p^2 P_{\mu\bar{\mu}, \nu\bar{\nu}}^{(-)}, \quad (3.10)$$

$$\sum_{\lambda} \langle 0 | \bar{q} T^A \sigma_{\mu\bar{\mu}} q | [1^{+-}](p, \lambda) \rangle \langle [1^{+-}](p, \lambda) | \bar{q} T^B \sigma_{\nu\bar{\nu}} q | 0 \rangle = -\delta^{AB} (f_+^T)^2 p^2 P_{\mu\bar{\mu}, \nu\bar{\nu}}^{(+)}, \quad (3.11)$$

which defines the projection operators as

$$P_{\mu\bar{\mu}; \nu\bar{\nu}}^{(-)} = g_{\mu\nu} \frac{p_{\bar{\mu}} p_{\bar{\nu}}}{p^2} + g_{\bar{\mu}\bar{\nu}} \frac{p_{\mu} p_{\nu}}{p^2} - g_{\bar{\mu}\nu} \frac{p_{\mu} p_{\bar{\nu}}}{p^2} - g_{\mu\bar{\nu}} \frac{p_{\bar{\mu}} p_{\nu}}{p^2}, \quad (3.12)$$

$$P_{\mu\bar{\mu}; \nu\bar{\nu}}^{(+)} = P_{\mu\bar{\mu}, \nu\bar{\nu}}^{(-)} + (g_{\mu\bar{\nu}} g_{\bar{\mu}\nu} - g_{\mu\nu} g_{\bar{\mu}\bar{\nu}}), \quad (3.13)$$

with the relation $[P^{(\pm)} P^{(\mp)}]_{\mu\bar{\mu}; \nu\bar{\nu}} = 0$. Considering the assumed symmetries, the four mesonic modes reside in the same symmetry group $U(2)_L \times U(2)_R$. The group structure allows the transformation among these modes depending on quantum numbers. For example, both the $\bar{\omega}$ state and the \bar{h}_1 state have isospin 0 and they can be transformed to each other through the $U_A(1)$ transformation. The same is true for the isospin-1 states, the $\bar{\rho}$ and the \bar{b}_1 . Similarly, the chiral partner states can be transformed to each other through the axial $SU(2)$ flavor rotation [16], namely, the pair of $\bar{\omega}$ and the \bar{b}_1 , and the pair of the $\bar{\rho}$ and the \bar{h}_1 .

If all the symmetries are conserved, there should be no correlation between the two different representations of mesonic states. However, when chiral symmetry is broken at low energy regime, the mesonic states can have overlaps. Since the vector (or chiral) representations of the ω and ρ states read

$$\omega : [I^G J^{PC} = 0^-(1^{--})] \rightarrow \langle 0 | \bar{q} T^0 \gamma_{\alpha} q | \omega(p, \lambda) \rangle = f_{\omega}^V \epsilon_{\alpha}^{(\lambda)}, \quad (3.14)$$

$$\rho : [I^G J^{PC} = 1^+(1^{--})] \rightarrow \langle 0 | \bar{q} T^a \gamma_{\alpha} q | \rho(p, \lambda) \rangle = f_{\rho^a}^V \epsilon_{\alpha}^{(\lambda)}, \quad (3.15)$$

the overlap between the vector and tensor representations can be described as

$$\sum_{\lambda} \langle 0 | \bar{q} T^A \gamma_{\alpha} q | [1^{--}](p, \lambda) \rangle \langle [1^{--}](p, \lambda) | \bar{q} T^B \sigma_{\mu\nu} q | 0 \rangle \simeq -i\delta^{AB} f_-^V f_-^T \mathcal{P}_{\alpha; \mu\nu}, \quad (3.16)$$

where $P_{\alpha; \mu\nu} = g_{\alpha\mu} p_{\nu} - g_{\alpha\nu} p_{\mu}$ projects only the transverse polarization. We also use the polarization sum in the $SU(2)_V$ diagonal phase, i.e., $\sum_{\lambda} \epsilon_{\alpha}^{(\lambda)} \bar{\epsilon}_{\mu}^{(\lambda)*} = -g_{\alpha\mu}$. Algebraic details for tensor currents and their transformations are presented in Appendix A.

3.2 b_1 meson decay in the soft pion limit

The $\bar{b}_1[1^+(1^{+-})]$ and $\bar{\omega}[0^-(1^{--})]$ mesonic states transform to each other under $SU(2)_L \times SU(2)_R$ symmetry. In the $SU(2)_V$ phase, if the $b_1(1235)$ meson state couples strongly to the tensor current ($\tilde{J}_{\mu\bar{\mu}}^a$), the overlap for the decay of $b_1(1235) \rightarrow \pi\omega(782)$ can be expressed as

$$\begin{aligned} \langle \pi^a(q)\omega(k') | i\tilde{J}_{\mu\bar{\mu}}^a(k) | 0 \rangle &\simeq f_{b_1}^T \sum_{\lambda} \langle \pi^a(q)\omega(k') | \bar{b}_1^a(k, \lambda) \rangle (\bar{\epsilon}_{\mu}^{(\lambda)*} k_{\bar{\mu}} - \bar{\epsilon}_{\bar{\mu}}^{(\lambda)*} k_{\mu}) \\ &\quad - f_{\rho}^T \sum_{\lambda} \langle \pi^a(q)\omega(k') | \bar{\rho}(k, \lambda) \rangle \frac{\bar{\epsilon}_{\mu\bar{\mu}\alpha\bar{\alpha}}}{2} (\bar{\epsilon}^{(\lambda)*\alpha} k_{\bar{\alpha}} - \bar{\epsilon}^{(\lambda)*\bar{\alpha}} k^{\alpha}) \\ &\quad + \dots, \end{aligned} \quad (3.17)$$

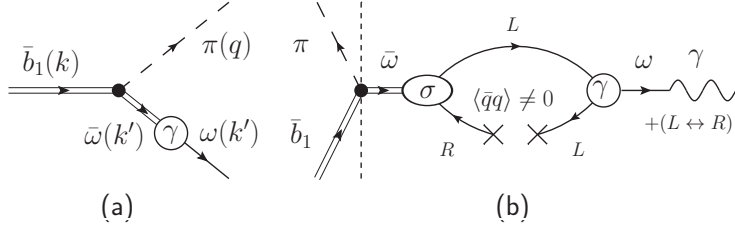


Figure 1. The \bar{b}_1 decay in chiral representation. (a) $\bar{b}_1 \rightarrow \pi\bar{\omega} \rightarrow \pi\omega$ via pion breaking and (b) $\bar{b}_1 \rightarrow \pi\gamma$ in the VMD hypothesis inferred from Eq. (3.21). Double lines denote the spin-1 mesonic states in tensor representation. The greek letters, ‘ σ ’ and ‘ γ ,’ in the blob represent the tensor and vector current representation, respectively.

where $\tilde{J}_{\mu\bar{\mu}}^a(k) \equiv -\frac{1}{2}\epsilon_{\mu\bar{\mu}\alpha\bar{\alpha}}(k^2 - \bar{m}^2) \int d^4x e^{ikx} \bar{q}(x) T^a \sigma^{\alpha\bar{\alpha}} q(x)$ with \bar{m} being the meson mass in the tensor representation. In the soft pion limit, the overlap can be rewritten as

$$\begin{aligned} \langle \pi^a(q)\omega(k') | i\tilde{J}_{\mu\bar{\mu}}^a(k) | 0 \rangle &= \frac{i}{f_\pi} \int d^3x e^{-i\mathbf{q}\cdot\mathbf{x}} \langle \omega(k') | [J_{50}^a(x), i\tilde{J}_{\mu\bar{\mu}}^a(k)] | 0 \rangle \\ &= \frac{i}{f_\pi} [-3i \langle \omega(k) | iJ_{\mu\bar{\mu}}^0(k) | 0 \rangle + R_1(q)] \\ &\simeq \frac{3f_\omega^T}{f_\pi} \sum_\lambda \langle \omega(k) | \bar{\omega}(k, \lambda) \rangle (\bar{\epsilon}_\mu^{(\lambda)*} k_{\bar{\mu}} - \bar{\epsilon}_{\bar{\mu}}^{(\lambda)*} k_\mu) + \dots, \end{aligned} \quad (3.18)$$

where $J_{\mu\bar{\mu}}^0(k) \equiv (k^2 - \bar{m}^2) \int d^4x e^{ikx} \bar{q}(x) T^0 \sigma^{\mu\bar{\mu}} q(x)$ and $R_1(q)$ represents $|\mathbf{q}|$ -dependent contributions in the limit of $\lim_{q \rightarrow 0} R_1(q) = 0$. Comparing Eqs. (3.17) and (3.18), the $|\mathbf{q}|$ -independent term can be obtained as

$$\lim_{q \rightarrow 0} \langle \pi^a(q)\omega(k') | \bar{b}_1^a(k, \lambda) \rangle \simeq \frac{3f_\omega^T}{f_\pi f_{b_1}^T} \langle \omega(k) | \bar{\omega}(k, \lambda) \rangle. \quad (3.19)$$

If the $\bar{\omega}$ is identified as the $\omega(782)$ state, one can obtain the strength for the $b_1 \rightarrow \pi\gamma$ decay from the overlap for $b_1 \rightarrow \pi\omega$ with the VMD hypothesis. This process can be written as the following current correlation function in the soft pion limit:

$$\begin{aligned} \langle \pi^a(q) | J_\alpha^0(k') i\tilde{J}_{\mu\bar{\mu}}^a(k) | 0 \rangle &= \frac{i}{f_\pi} \int d^3x e^{-i\mathbf{q}\cdot\mathbf{x}} \langle 0 | [J_{50}^a(x), J_\alpha^0(k) i\tilde{J}_{\mu\bar{\mu}}^a(k)] | 0 \rangle \\ &= \frac{i}{f_\pi} [\langle 0 | [Q_5^a, J_\alpha^0(k) i\tilde{J}_{\mu\bar{\mu}}^a(k)] | 0 \rangle + \langle 0 | J_\alpha^0(k) [Q_5^a, i\tilde{J}_{\mu\bar{\mu}}^a(k)] | 0 \rangle \\ &\quad + R_2(q)] \\ &= \frac{i}{f_\pi} [-3i \langle 0 | J_\alpha^0(k) iJ_{\mu\bar{\mu}}^0(k) | 0 \rangle + \dots] \\ &\simeq \frac{3f_\omega f_\omega^T}{f_\pi} \sum_\lambda \langle \omega(k, \lambda) | \bar{\omega}(k, \lambda) \rangle \epsilon_\alpha^{(\lambda)} (\bar{\epsilon}_\mu^{(\lambda)*} k_{\bar{\mu}} - \bar{\epsilon}_{\bar{\mu}}^{(\lambda)*} k_\mu) + \dots, \end{aligned} \quad (3.20)$$

where $J_\alpha^0(k) \equiv (k^2 - m^2) \int d^4x e^{ikx} \bar{q}(x) T^0 \gamma_\alpha q(x)$ with m being the meson mass in chiral representation and $R_2(q)$ represents the $|\mathbf{q}|$ -dependent contributions with the condition

that $\lim_{q \rightarrow 0} R_2(q) = 0$. The overlap $f_\omega f_\omega^T \langle \omega(k, \lambda) | \bar{\omega}(k, \lambda) \rangle$ can be calculated from the time-ordered correlator as

$$\Pi^{\bar{b}_1 - \pi \omega}(k) = \frac{3}{f_\pi} \int d^4x e^{ikx} \langle \mathcal{T} [J_\alpha^0(x) J_{\mu\bar{\mu}}^0(0)] \rangle. \quad (3.21)$$

If chiral symmetry is restored, the correlation (3.21) will vanish because the representation spaces of currents are totally disconnected. Diagrammatical descriptions of this process are depicted in Fig. 1. Therefore, Eq. (3.20) describes the decay mechanism of $\bar{b}_1 \rightarrow \pi \gamma$ that evades the usual VMD hypothesis. Then, the interpretation of the \bar{b}_1 and $\bar{\omega}$ is required in connection with physical states, namely, to see whether and how the tensor representation can describe observed mesons.

4 Operator product expansion and spectral sum rules

Understanding the nature of the $\bar{\omega}$ and \bar{b}_1 states requires their relations to the physical $\omega(782)$ and $b_1(1235)$ mesons. For this purpose, we analyze the spectral sum rules for the corresponding masses of these mesonic states. The correlation function can be calculated via OPE in the $k^2 \rightarrow -\infty$ limit as in Refs. [17, 20–25].

4.1 OPE of the correlators

To interpolate the mesonic state with given quantum numbers we employ the tensor current,

$$J_{\mu\bar{\mu}}^A(x) = \bar{q}(x) T^A \sigma_{\mu\bar{\mu}} q(x), \quad (4.1)$$

where flavor matrix T^0 corresponds to the $(\bar{\omega}, \bar{h}_1)$ current and T^a corresponds to $(\bar{\rho}^a, \bar{b}_1^a)$ current. The correlator can be obtained as [24, 25]

$$\begin{aligned} \Pi_{\mu\bar{\mu};\nu\bar{\nu}}^{AB}(k) &= i \int d^4x e^{ikx} \langle \mathcal{T} [\bar{q}(x) T^A \sigma_{\mu\bar{\mu}} q(x) \bar{q}(0) T^B \sigma_{\nu\bar{\nu}} q(0)] \rangle \\ &= \Pi_-^{\text{ope}}(k^2) P_{\mu\bar{\mu};\nu\bar{\nu}}^{(-)} + \Pi_+^{\text{ope}}(k^2) P_{\mu\bar{\mu};\nu\bar{\nu}}^{(+)}, \end{aligned} \quad (4.2)$$

$$\Pi_{\mp}^{\text{ope}}(k^2) = \frac{\delta^{AB}}{2} \left[\Pi_{\text{pert.}}(k^2) + \Pi_{G^2}(k^2) \pm \Pi_{4q(a)}^A(k^2) + \Pi_{4q(b)}(k^2) \right], \quad (4.3)$$

where nonzero OPE terms are found as

$$\Pi_{\text{pert.}}(k^2) = \frac{1}{8\pi^2} (-k^2) \left[\left(1 + \frac{7\alpha_s}{9\pi} \right) \ln(-k^2/\mu^2) + \frac{\alpha_s}{3\pi} (\ln(-k^2/\mu^2))^2 \right], \quad (4.4)$$

$$\Pi_{G^2}(k^2) = \frac{1}{24} \left(-\frac{1}{k^2} \right) \left\langle \frac{\alpha_s}{\pi} G^2 \right\rangle, \quad (4.5)$$

$$\Pi_{4q(a)}^A(k^2) = -32\pi\alpha_s \left(-\frac{1}{k^2} \right)^2 \left(\langle \bar{q} T^A \tau^{\bar{a}} q \bar{q} T^A \tau^{\bar{a}} q \rangle + \langle \bar{q} T^A \tau^{\bar{a}} \gamma_5 q \bar{q} T^A \tau^{\bar{a}} \gamma_5 q \rangle \right), \quad (4.6)$$

$$\Pi_{4q(b)}(k^2) = -\frac{8\pi\alpha_s}{9} \left(-\frac{1}{k^2} \right)^2 \langle \bar{q} T^0 \tau^{\bar{a}} \gamma_\eta q \bar{q} T^0 \tau^{\bar{a}} \gamma^\eta q \rangle, \quad (4.7)$$

with $G_{\rho\sigma} = D_\rho A_\sigma - D_\sigma A_\rho$ being the gluon field strength tensor and $\mu = 0.5$ GeV is the OPE separation scale where the condensate is normalized.⁷ The correlator (3.21) can be calculated as

$$\begin{aligned}\Pi_{\alpha;\mu\bar{\mu}}^{\bar{b}_1-\pi\omega}(k) &= \frac{3}{f_\pi} \int d^4x e^{ikx} \langle \mathcal{T}[\bar{q}(x)T^0\gamma_\alpha q(x)\bar{q}(0)T^0\sigma_{\mu\bar{\mu}}q(0)] \rangle \\ &= \Pi^{\bar{b}_1-\pi\omega}(k^2) P_{\alpha;\mu\bar{\mu}}^{(\gamma-\sigma)},\end{aligned}\quad (4.8)$$

where

$$\Pi^{\bar{b}_1-\pi\omega}(k^2) = -\frac{3}{f_\pi} \left\{ -\frac{1}{k^2} \langle \bar{q}T^0 q \rangle + \frac{1}{12} \left(-\frac{1}{k^2} \right)^2 \langle \bar{q}T^0 g\sigma \cdot Gq \rangle \right\}.\quad (4.9)$$

4.2 Spectral sum rules

The invariants can be weighted to emphasize the ground state contribution as follows:

$$\begin{aligned}\mathcal{W}_M^{\text{subt.}}[\Pi_{\mp}^{\text{ope}}(k^2)] &= \frac{1}{\pi} \int_0^{s_0} ds e^{-s/M^2} \text{Im}[\Pi_{\mp}^{\text{ope}}(s)] \\ &= -\frac{1}{16\pi^2} \left[\left(1 + \frac{7\alpha_s}{9\pi} \right) (M^2)^2 E_1(s_0) + \frac{\alpha_s}{3\pi} L(s_0) \right] \\ &\quad \mp \frac{16\pi\alpha_s}{M^2} (\langle \bar{q}T^A\tau^{\bar{a}}q\bar{q}T^A\tau^{\bar{a}}q \rangle + \langle \bar{q}T^A\tau^{\bar{a}}\gamma_5q\bar{q}T^A\tau^{\bar{a}}\gamma_5q \rangle) \\ &\quad - \frac{4\pi\alpha_s}{9M^2} \langle \bar{q}T^0\tau^{\bar{a}}\gamma_\eta q\bar{q}T^0\tau^{\bar{a}}\gamma_\eta q \rangle - \frac{1}{48} \left\langle \frac{\alpha_s}{\pi} G^2 \right\rangle,\end{aligned}\quad (4.10)$$

where ‘ \mp ’ denote parity-odd and parity-even modes and the OPE continuum contribution ($k^2 > s_0$), where the excited states are assumed, is subtracted as

$$E_1(s_0) \equiv 1 - e^{-s_0/M^2} (1 + s_0/M^2).\quad (4.11)$$

We also define

$$L(s_0) \equiv 2 \int_0^{s_0} ds e^{-s/M^2} s \ln(s/\mu^2).\quad (4.12)$$

Detailed arguments for the weighting scheme are given in Appendix B. The strong coupling $\alpha_s = 0.5$ is obtained at the separation scale $\mu = 0.5$ GeV with $\Lambda_{\text{QCD}} = 0.125$ GeV. After Borel weighting, α_s is kept as constant.

The value of the gluon condensate is taken as $\langle (\alpha_s/\pi)G^2 \rangle = (0.33 \text{ GeV})^4$ [20–22]. By using the factorization hypothesis,

$$\langle q_\alpha \bar{q}_\beta q_\gamma \bar{q}_\delta \rangle_{\rho,I} \simeq \langle q_\alpha \bar{q}_\beta \rangle_{\rho,I} \langle q_\gamma \bar{q}_\delta \rangle_{\rho,I} - \langle q_\alpha \bar{q}_\delta \rangle_{\rho,I} \langle q_\gamma \bar{q}_\beta \rangle_{\rho,I},\quad (4.13)$$

where the color indices are omitted, the four-quark condensates are estimated in factorized forms as

$$\langle \bar{q}T^A\tau^{\bar{a}}q\bar{q}T^A\tau^{\bar{a}}q \rangle \rightarrow -\frac{\alpha_A}{18} \langle \bar{q}T^0q \rangle_{\text{vac}}^2,\quad (4.14)$$

$$\langle \bar{q}T^A\tau^{\bar{a}}\gamma_5q\bar{q}T^A\tau^{\bar{a}}\gamma_5q \rangle \rightarrow -\frac{\beta_A}{18} \langle \bar{q}T^0q \rangle_{\text{vac}}^2,\quad (4.15)$$

$$\langle \bar{q}T^0\tau^{\bar{a}}\gamma_\eta q\bar{q}T^0\tau^{\bar{a}}\gamma_\eta q \rangle \rightarrow -\frac{2\gamma}{9} \langle \bar{q}T^0q \rangle_{\text{vac}}^2,\quad (4.16)$$

⁷In Eq. (4.6), the index A is not summed over.

where $\langle \bar{q}T^0 q \rangle_{\text{vac}}$ is obtained from the Gellmann-Oakes-Renner relation [19],

$$2m_q \langle \bar{q}T^0 q \rangle_{\text{vac}} = -m_\pi^2 f_\pi^2, \quad (4.17)$$

with $m_\pi = 138$ MeV and $f_\pi = 93$ MeV. This leads to $\langle \bar{q}T^0 q \rangle_{\text{vac}} \simeq -(254 \text{ MeV})^3$ for $m_q = 5$ MeV. The parameters in Eqs. (4.14)-(4.16) have the same value, namely, $\alpha_A = \beta_A = \gamma = 1$, in the usual factorization hypothesis. Hereafter, each parameter set with explicit isospin dependence, i.e., α_0 , β_0 , α_a , and β_a with $a = 1, 2, 3$, represents the factorization of the isoscalar and isovector four-quark condensates, respectively. The anomalous running of $\langle \bar{q}T^0 q \rangle_{\text{vac}}^2$ is neglected because the factorization scheme is used only for estimating the four-quark condensate scale. Various scales of α , β , and γ are assumed in the present work to include variations coming from the running of the condensates. As can be seen from Eqs. (4.14)-(4.16), the four quark condensates can be written as a product of two quark antiquark pair. Depending on the color and flavor matrices appearing in the quark antiquark pair, the factorization parameters α , β , γ can take different values. This is so because, when there is an isospin operator in the quark antiquark pair, the quark-disconnected diagrams vanish identically. Furthermore, even for isosinglet quark antiquark pair, depending on the chiral and color structure, the quark-disconnected diagrams are expected to have different contributions. Therefore, in the present work, we choose the parameter set taking into account the following three conditions depending on the color and isospin structure of the quark antiquark pair: (a) possible correlation types that depend on chiral symmetry breaking, (b) nontrivial topological contribution from color gauge group, and (c) stability of the Borel curves. For isovector quark-antiquark pair, the usual factorization provides quark-connected-like condensates. The condensates are given in the local limit of the pair of gauge equivalent nonlocal bilinear [26]. The colored pieces are part of the Dirac eigenmodes in the nonlocal gauge equivalent structure of the mesonic current. So the isoscalar condensates are considered to have nonzero quark-disconnected-like contribution if the colored spinless bilinear appears in pair to produce the totally color singlet configuration. Considering the possibility of this contribution, which does not appear in the usual factorization scheme, the quark-disconnected-like and quark-connected-like contributions are encoded in the isoscalar and isovector parameters, respectively. This typically leads to $|\alpha_0| < |\alpha_a|$ and $|\beta_0| < |\beta_a|$. Also, if one considers topologically nontrivial gauge contributions, the spinless but parity-odd combination of quark bilinear can have nonzero correlation in the same way as argued in Refs. [28, 29]. For the condensate composed with pseudoscalar bilinear in Eq. (4.16), the nontrivial contribution may appear as an alternating series in winding number of the color gauge. Sum rule analysis with the parameters taken according to these criteria are found to produce stable Borel curves.

We first take $(\alpha_0 = 0.8, \alpha_a = 1.0)$ as the reference parameter set, which is similar to the usual factorization.⁸ To ensure that the ground state contribution becomes dominant and

⁸We leave short technical remarks for the sum rules. Some parameter sets with $(\alpha_A < 0, \beta_A < 0)$ are found to give a mass of the parity-odd mode close to ~ 800 MeV. However, these parameter sets lead to unstable Borel curves and controversial results for the parity-even mode sum rules. Therefore, we do not adopt these parameter sets in our study. More detailed sum rules analyses for $\bar{\omega}$ and \bar{b}_1 states with $(a_A < 0, b_A < 0)$ are reported in Appendix B.

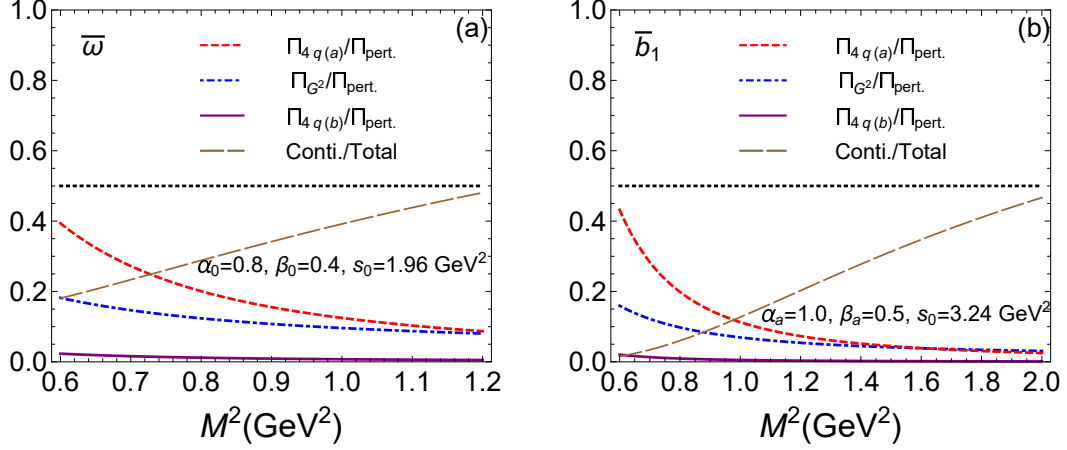


Figure 2. Spectral structure of the weighted invariant (a) for the $\bar{\omega}$ and (b) for the \bar{b}_1 . As a reference, black dotted lines are given to denote 50%.

the OPEs are convergent, the Borel windows for the $\bar{\omega}$ and \bar{b}_1 sum rules are chosen to be in the range of $0.6 \text{ GeV}^2 < M^2 < 1.2 \text{ GeV}^2$ and $0.6 \text{ GeV}^2 < M^2 < 2.0 \text{ GeV}^2$, respectively. Plotted in Fig. 2 are spectral structures of the invariants.

If the ground state is the one-particle mesonic state as explained in Sec. 3, the phenomenological structure can be written as

$$\begin{aligned} \Pi_{\mp}^{\text{ph.pole}}(k^2) &= \frac{(f_{\mp}^T)^2 k^2}{k^2 - m_{\mp}^2 + i\epsilon} \\ &= \mathcal{P} \frac{(f_{\mp}^T)^2 k^2}{(k^2 - m_{\mp}^2)} - i\pi (f_{\mp}^T)^2 k^2 \delta(k^2 - m_{\mp}^2). \end{aligned} \quad (4.18)$$

However, it is also possible that the tensor current (4.1) can couple to some kinds of hybrid states, which are composed of two particles, if the mass scale of the hybrid is compatible with the one-particle mesonic state. The hybrid state containing the quantum number of the ω meson can be inferred from the anomalous interaction that is written as [10]

$$\mathcal{L}_{\omega\pi\rho}^{\epsilon 1} = \frac{g_{\omega\pi\rho}}{2} \epsilon^{\mu\bar{\mu}\alpha\bar{\alpha}} \omega_{\mu\bar{\mu}} \partial_{\alpha} \pi^a \rho_{\bar{\alpha}}^a = -g_{\omega\pi\rho} \epsilon^{\mu\bar{\mu}\alpha\bar{\alpha}} \omega_{\bar{\mu}} \partial_{\alpha} \pi^a \partial_{\mu} \rho_{\bar{\alpha}}^a, \quad (4.19)$$

where $\omega_{\mu\bar{\mu}}$ is the ω field strength tensor. As the ω and $\bar{\omega}$ states share the same quantum numbers $[0^-(1^-)]$, the phenomenological interpolating current for the $\bar{\omega}$ state can be written as

$$J_{\mu\bar{\mu}}^{\bar{\omega}}(x) \equiv \epsilon_{\mu\bar{\mu}\alpha\bar{\alpha}} \text{Tr} [\partial^{\alpha} \pi(x) \rho^{\bar{\alpha}}(x)], \quad (4.20)$$

where the trace is summed over flavor indices. The corresponding phenomenological struc-

ture of $\Pi_{(\mp)}^{\bar{\omega}}(k^2)$ can be obtained from the correlator of $J_{\mu\bar{\mu}}^{\bar{\omega}}$ as

$$\begin{aligned}
\Pi_{\mu\bar{\mu};\nu\bar{\nu}}^{\bar{\omega}}(k) &= i \int d^4x e^{ikx} \left\langle \mathcal{T} \left[\epsilon_{\mu\bar{\mu}\alpha\bar{\alpha}} \text{Tr} [\partial^\alpha \pi(x) \rho^{\bar{\alpha}}(x)] \epsilon_{\nu\bar{\nu}\beta\bar{\beta}} \text{Tr} [\partial^\beta \pi(0) \rho^{\bar{\beta}}(0)] \right] \right\rangle \\
&= \frac{3i}{4} \epsilon_{\mu\bar{\mu}\alpha\bar{\alpha}} \epsilon_{\nu\bar{\nu}\beta\bar{\beta}} \int \frac{d^4p}{(2\pi)^4} \frac{(p+k)^\alpha (p+k)^\beta}{(p+k)^2 - m_\pi^2} \frac{1}{p^2 - m_\rho^2} \left(g^{\bar{\alpha}\bar{\beta}} - \frac{p^{\bar{\alpha}} p^{\bar{\beta}}}{m_\rho^2} \right) \\
&= \Pi_-^{\bar{\omega}}(k^2) P_{\mu\bar{\mu};\nu\bar{\nu}}^{(-)} + \Pi_+^{\bar{\omega}}(k^2) P_{\mu\bar{\mu};\nu\bar{\nu}}^{(+)}, \tag{4.21}
\end{aligned}$$

where m_ρ is the ρ meson mass and the invariant function for each parity mode can be calculated as

$$\begin{aligned}
\Pi_-^{\bar{\omega}}(k^2) &= \frac{3}{4(4\pi)^2} \int_0^1 dx \left(-x(1-x)k^2 + (1-x)m_\rho^2 \right) \ln \left(-x(1-x)k^2 + (1-x)m_\rho^2 \right) \\
&\quad + R_-(k^2), \tag{4.22}
\end{aligned}$$

$$\begin{aligned}
\Pi_+^{\bar{\omega}}(k^2) &= \frac{3}{4(4\pi)^2} \int_0^1 dx \left[- (1-x)^2 k^2 + \left(x \left(1 - \frac{x}{2} \right) \frac{k^2}{m^2} - 1 \right) \left(-x(1-x)k^2 + (1-x)m_\rho^2 \right) \right] \\
&\quad \times \ln \left[-x(1-x)k^2 + (1-x)m_\rho^2 \right] + R_+(k^2), \tag{4.23}
\end{aligned}$$

where $R_{\mp}(k^2)$ is a regular polynomial and the $m_\pi \rightarrow 0$ limit has been taken. One can verify that the imaginary part appears in the range of $m_\rho^2/k^2 < x < 1$. The weighted $\Pi_-^{\bar{\omega}}(k^2)$ can be obtained as

$$\begin{aligned}
\mathcal{W}_M^{\text{subt.}} [\Pi_-^{\bar{\omega}}(k^2)] &= \frac{1}{\pi} \int_{m_\rho^2}^{s_0} ds e^{-s/M^2} \text{Im} [\Pi_-^{\bar{\omega}}(s)] \\
&= \frac{3}{64\pi^2} \int_{m_\rho^2}^{s_0} ds e^{-s/M^2} \left(-\frac{s}{6} + \frac{m_\rho^2}{2} - \frac{1}{2} \frac{(m_\rho^2)^2}{s} + \frac{1}{6} \frac{(m_\rho^2)^3}{s^2} \right) \\
&= \frac{3}{64\pi^2} \left\{ \frac{M^2}{6} \left(s_0 e^{-s_0/M^2} - m_\rho^2 e^{-m_\rho^2/M^2} \right) + \frac{(M^2)^2}{6} \left(e^{-s_0/M^2} - e^{-m_\rho^2/M^2} \right) \right. \\
&\quad - \frac{m_\rho^2}{2} M^2 \left(e^{-s_0/M^2} - e^{-m_\rho^2/M^2} \right) \\
&\quad - \frac{(m_\rho^2)^2}{2} \left[\Gamma(0, m_\rho^2/M^2) - \Gamma(0, s_0/M^2) \right] \\
&\quad - \frac{(m_\rho^2)^3}{6} \left[\frac{e^{-s_0/M^2}}{s_0} - \frac{e^{-m_\rho^2/M^2}}{m_\rho^2} \right. \\
&\quad \left. \left. + \frac{1}{M^2} \left\{ \Gamma(0, m_\rho^2/M^2) - \Gamma(0, s_0/M^2) \right\} \right] \right\}, \tag{4.24}
\end{aligned}$$

where the continuum threshold s_0 is taken to be the same as that assigned in $\mathcal{W}_M^{\text{subt.}}[\Pi_-^{\text{ope}}(k^2)]$, and $\Gamma(t, x) = \int_x^\infty ds s^{t-1} e^{-s}$ is the incomplete Gamma function.

Similarly, the loop-like phenomenological current for \bar{b}_1 state can be defined as

$$J_{\mu\bar{\mu}}^{\bar{b}_1 a}(x) \equiv \frac{\sqrt{3}}{2} \epsilon_{\mu\bar{\mu}\alpha\bar{\alpha}} \partial^\alpha \pi^a(x) \omega^{\bar{\alpha}}(x). \tag{4.25}$$

The corresponding invariant can be obtained from the parity-even mode of Eq. (4.23) by replacing m by m_ω . The imaginary part appears in the range of $m_\omega^2/k^2 < x < 1$ and the weighted $\Pi_+^{\bar{b}_1}(k^2)$ is analogously obtained as

$$\begin{aligned}
\mathcal{W}_M^{\text{subt.}} \left[\Pi_+^{\bar{b}_1}(k^2) \right] &= \frac{1}{\pi} \int_{m_\omega^2}^{s_0} ds e^{-s/M^2} \text{Im} \left[\Pi_+^{\bar{b}_1}(s) \right] \\
&= \frac{3}{64\pi^2} \int_{m_\omega^2}^{s_0} ds e^{-s/M^2} \left(-\frac{1}{6} \frac{s^2}{m_\omega^2} - \frac{s}{6} + \frac{m_\omega^2}{4} + \frac{1}{3} \frac{(m_\omega^2)^2}{s} - \frac{1}{4} \frac{(m_\omega^2)^3}{s^2} + \frac{1}{10} \frac{(m_\omega^2)^4}{s^3} \right) \\
&= \frac{3}{64\pi^2} \left\{ \frac{1}{6} \frac{M^2}{m_\omega^2} \left(s_0^2 e^{-s_0/M^2} - (m_\omega^2)^2 e^{-m_\omega^2/M^2} \right) + \frac{1}{3} \frac{(M^2)^2}{m_\omega^2} \left(s_0 e^{-s_0/M^2} - m_\omega^2 e^{-m_\omega^2/M^2} \right) \right. \\
&\quad + \frac{1}{3} \frac{(M^2)^3}{m_\omega^2} \left(e^{-s_0/M^2} - e^{-m_\omega^2/M^2} \right) + \frac{M^2}{6} \left(s_0 e^{-s_0/M^2} - m_\omega^2 e^{-m_\omega^2/M^2} \right) \\
&\quad + \frac{(M^2)^2}{6} \left(e^{-s_0/M^2} - e^{-m_\omega^2/M^2} \right) - \frac{m_\omega^2}{4} \left[M^2 \left(e^{-s_0/M^2} - e^{-m_\omega^2/M^2} \right) \right] \\
&\quad + \frac{(m_\omega^2)^2}{3} \left[\Gamma(0, m_\omega^2/M^2) - \Gamma(0, s_0/M^2) \right] \\
&\quad + \frac{(m_\omega^2)^3}{4} \left[\frac{e^{-s_0/M^2}}{s_0} - \frac{e^{-m_\omega^2/M^2}}{m_\omega^2} + \frac{1}{M^2} \left[\Gamma(0, m_\omega^2/M^2) - \Gamma(0, s_0/M^2) \right] \right] \\
&\quad \left. - \frac{(m_\omega^2)^4}{20} \left[\frac{e^{-s_0/M^2}}{s_0^2} - \frac{e^{-m_\omega^2/M^2}}{(m_\omega^2)^2} - \frac{1}{M^2} \left(\frac{e^{-s_0/M^2}}{s_0} - \frac{e^{-m_\omega^2/M^2}}{m_\omega^2} \right) \right. \right. \\
&\quad \quad \left. \left. - \left(\frac{1}{M^2} \right)^2 \left(\Gamma(0, m_\omega^2/M^2) - \Gamma(0, s_0/M^2) \right) \right] \right\}. \tag{4.26}
\end{aligned}$$

Then the sum rule for the ground states interpolated by the tensor current reads

$$\mathcal{W}_M^{\text{subt.}} \left[\Pi_\mp^{\text{ope}}(k^2) \right] = -(f_\mp^T)^2 m_\mp^2 e^{-m_\mp^2/M^2} + (c_\mp^{\text{hy.}})^2 \mathcal{W}_M^{\text{subt.}} \left[\Pi_\mp^{\text{hy.}}(k^2) \right], \tag{4.27}$$

where $c_\mp^{\text{hy.}}$ represents the coupling between the tensor current (4.1) and the hybrid state. Equation (4.27) leads to the hybrid-subtracted mass sum rules as

$$m_\mp = M^2 \left(\frac{(\partial/\partial M^2) \left(\mathcal{W}_M^{\text{subt.}} \left[\Pi_\mp^{\text{ope}}(k^2) \right] - (c_\mp^{\text{hy.}})^2 \mathcal{W}_M^{\text{subt.}} \left[\Pi_\mp^{\text{hy.}}(k^2) \right] \right)}{\mathcal{W}_M^{\text{subt.}} \left[\Pi_\mp^{\text{ope}}(k^2) \right] - (c_\mp^{\text{hy.}})^2 \mathcal{W}_M^{\text{subt.}} \left[\Pi_\mp^{\text{hy.}}(k^2) \right]} \right)^{\frac{1}{2}}. \tag{4.28}$$

By assuming only the one-particle meson state for the ground state, the obtained masses of the $\bar{\omega}$ and \bar{b}_1 modes are plotted respectively in Figs. 3(a) and 3(b). Depending on the values of α_0 and β_0 , the mass of the isoscalar parity-odd mode is found to vary from 1.0 GeV to 1.2 GeV, which is much higher than the physical $\omega(782)$ mass. On the other hand, the mass of the isovector parity-even mode shows weak dependence on the parameter set, and is in good agreement with the physical $b_1(1235)$ mass when $(\alpha_a = 1, \beta_a = 0.5)$ is employed. Presented in Figs. 3(c) and 3(d) are the mass curves for the cases where these parameters are larger than 1. In this case, the mass curves of the isoscalar parity-odd mode become

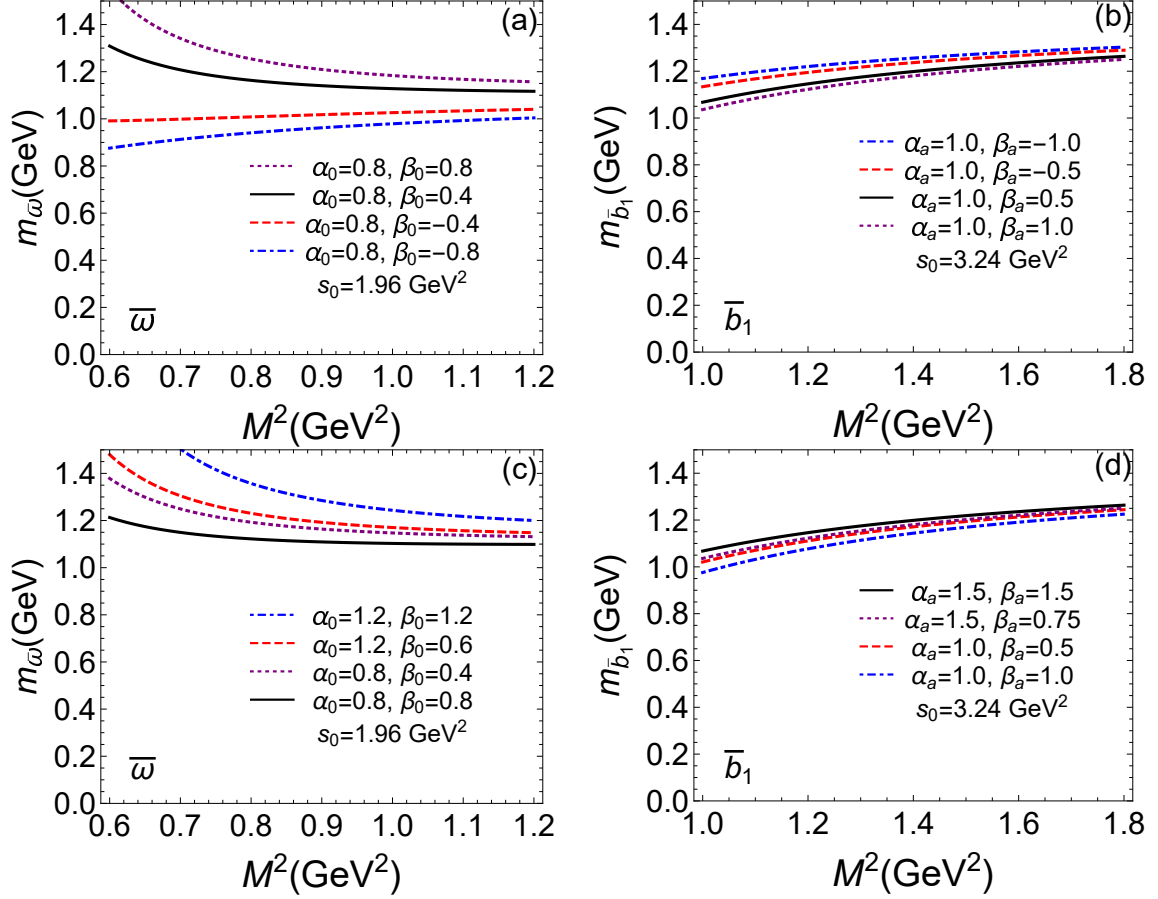


Figure 3. Mass sum rules for spin-1 meson states interpolated by the tensor current ($c = 1$). (a,c) isoscalar parity-odd channel ($\bar{\omega}$) with $s_0 = 1.96 \text{ GeV}^2$ and (b,d) isovector parity-even channel (\bar{b}_1) with $s_0 = 3.24 \text{ GeV}^2$.

larger than 1.2 GeV and unstable. On the other hand, the mass curves of isovector parity-even mode are not drastically changed. Because of the large mass difference between the $\omega(782)$ and $\bar{\omega}$, it is unnatural to identify the $\bar{\omega}$ state as the physical $\omega(782)$.

Considering the mass range determined by the Borel curve in Fig. 3(a) and the quantum numbers $[0^-(1^{--})]$, one may imagine that the adopted current couples to excited ω resonance states. However, such possibility is unlikely as the mass of the lowest excited state $\omega(1420)$ [1] is much larger than the mass range obtained in the sum rules analysis for the $\bar{\omega}$. Therefore, we explore the possibility that the employed current couples to a hybrid state composed of two particles. If the tensor current (4.1) strongly couples to the one-particle mesonic state (hybrid state), the sum rules for the one-particle meson pole residue f_{\mp}^T (the tensor current-hybrid coupling c_{\mp}^{hy}) should provide a stable behavior in the

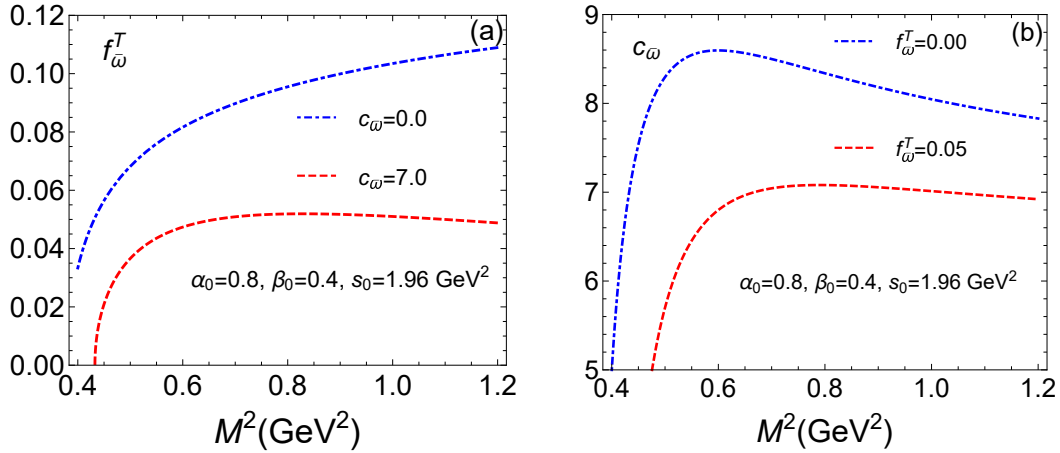


Figure 4. Borel curve (a) for the meson pole residue $f_{\bar{\omega}}^T$ and (b) for the tensor current-hybrid coupling $c_{\bar{\omega}}^{\text{hy.}}$.

Borel window. The sum rules for each coupling obtained from Eq. (4.27) read

$$f_{\mp}^T = \left\{ \frac{1}{m_{\mp}^2} e^{m_{\mp}^2/M^2} \left(-\mathcal{W}_M^{\text{subt.}} [\Pi_{\mp}^{\text{ope}}(k^2)] + (c_{\mp}^{\text{hy.}})^2 \mathcal{W}_M^{\text{subt.}} [\Pi_{\mp}^{\text{hy.}}(k^2)] \right) \right\}^{\frac{1}{2}}, \quad (4.29)$$

$$c_{\mp}^{\text{hy.}} = \left\{ \left(\mathcal{W}_M^{\text{subt.}} [\Pi_{\mp}^{\text{ope}}(k^2)] + (f_{\mp}^T)^2 m_{\mp}^2 e^{-m_{\mp}^2/M^2} \right) / \mathcal{W}_M^{\text{subt.}} [\Pi_{\mp}^{\text{hy.}}(k^2)] \right\}^{\frac{1}{2}}, \quad (4.30)$$

where m_{\mp}^2 , f_{\mp}^T , and $c_{\mp}^{\text{hy.}}$ are input parameters. If the one-particle pole is dominant in the ground state, the Borel curve for $f_{\bar{\omega}}^T$ will be stable. However, as can be seen in Fig. 4(a), the Borel curve is not stable, suggesting that something is missing or the assumption is not correct. On the other hand, $c_{\bar{\omega}}^{\text{hy.}}$ provides relatively stable behavior in the proper Borel window even with the no-pole scenario ($f_{\bar{\omega}}^T = 0$) and provides a plateau value $c_{\bar{\omega}}^{\text{hy.}} \simeq 7.0$ with $f_{\bar{\omega}}^T = 0.05$ as shown in Fig. 4(b). In these optimized curves, $f_{\bar{\omega}}^T$ reduces to 50% of its original scale when $c_{\bar{\omega}}^{\text{hy.}}$ is varied from 0 to 7.0, while $c_{\bar{\omega}}^{\text{hy.}}$ reduces only to 85% of its original scale when $f_{\bar{\omega}}^T$ varies from 0 to 0.05. This leads to the conclusion that the ground state information in the tensor current correlator is dominated by the hybrid state.

The \bar{b}_1 state can be analyzed in a similar way. As shown in Fig. 5, the Borel curves for the couplings in the \bar{b}_1 state shows the opposite tendency in comparison with the $\bar{\omega}$ analyses. Namely, the computed $f_{\bar{b}_1}^T$ values show plateau-like behavior even in the no-continuum condition ($c_{\bar{b}_1}^{\text{hy.}} = 0.0$) and reduces only to 90% of its original scale when $c_{\bar{b}_1}^{\text{hy.}} = 0.5$ is assigned. It is also found that $c_{\bar{b}_1}^{\text{hy.}}$ strongly depends on $f_{\bar{b}_1}^T$ variation and shows singular behavior when $f_{\bar{b}_1}^T > 0.11$ is assigned. Therefore, the \bar{b}_1 state is identified as the physical $b_1(1235)$ meson state considering the mass scale shown in Fig. 3(b).

By assuming only the π - ρ hybrid (i.e., the $\bar{\omega}$) or $b_1(1235)$ state for the ground state, the corresponding coupling sum rules are plotted in Fig. 6(a) and Fig. 6(b), respectively. We also found that $c_{\bar{\omega}}^{\text{hy.}}$ with $f_{\bar{\omega}}^T = 0$ shows stable Borel behavior and the plateau scale becomes moderate when $s_0 \geq 1.44 \text{ GeV}^2$, which means that the $\bar{\omega}$ state can be interpreted

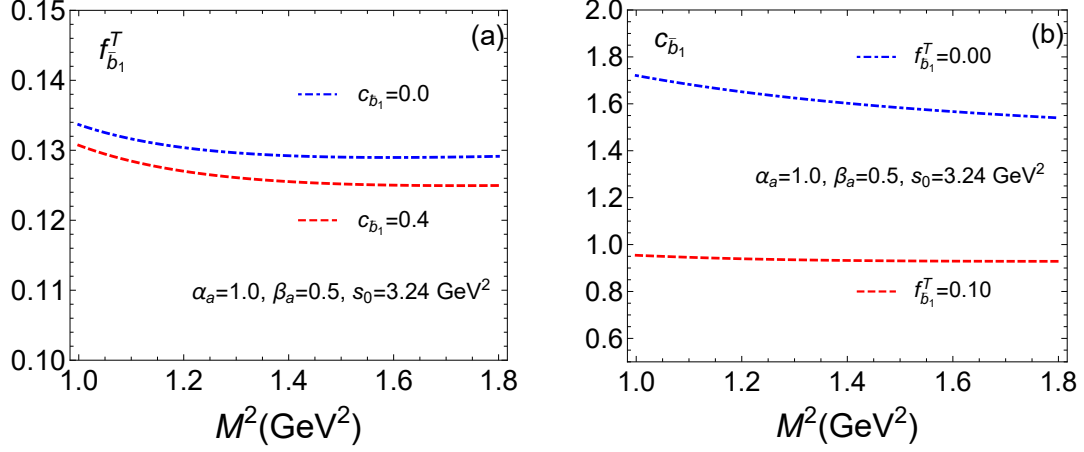


Figure 5. Borel curve (a) for the meson pole residue $f_{b_1}^T$ and (b) for the tensor current-hybrid coupling $c_{b_1}^{\text{hy}}$.

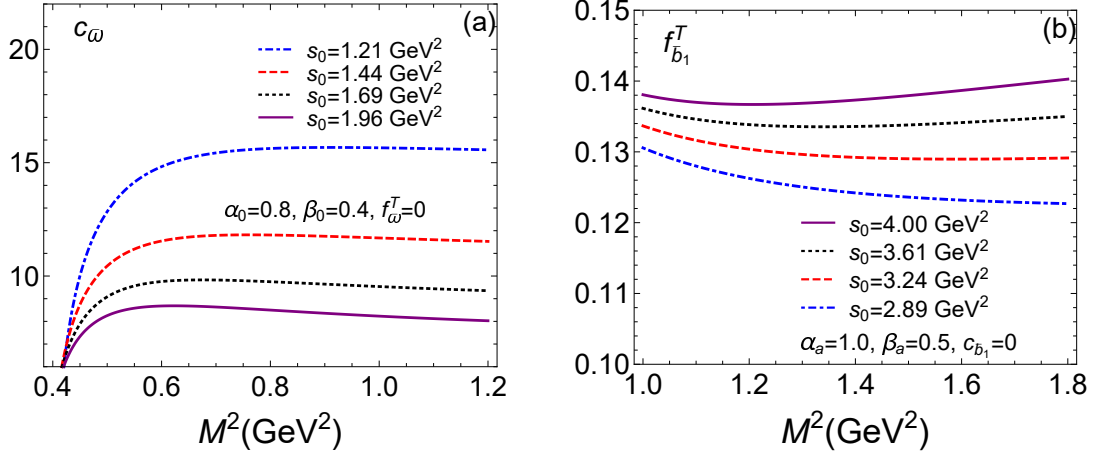


Figure 6. Coupling constants sum rules for (a) the tensor current-hybrid coupling c_{ω}^{hy} ($f_{\omega}^T = 0.00$) and (b) the meson pole residue $f_{b_1}^T$ ($c_{b_1}^{\text{hy}} = 0.0$) in various continuum thresholds.

as a hybrid state. Analogously, since $f_{b_1}^T$ with $c_{b_1}^{\text{hy}} = 0$ provides a plateau structure and the plateau scale becomes moderate when $s_0 \geq 3.24 \text{ GeV}^2$, the one particle $b_1(1235)$ state would be good enough to approximate the \bar{b}_1 state.

5 Discussion and Conclusion

The $b_1(1235)$ meson state mostly decays into the $\pi\omega$ state by the strong interactions and the $\pi\gamma$ state by the electromagnetic interactions. As the VMD scenario is successful in explaining the decays and form factors of ground state hadrons, low-energy phenomenology usually assumes that the photon always sees hadrons through vector meson states [6, 7, 13, 14]. However, for the electromagnetic decays of the $b_1(1235)$ meson, the VMD hypothesis is not enough to explain the measured $\Gamma(b_1 \rightarrow \pi\gamma)$ [13, 14]. In the present work, we explore

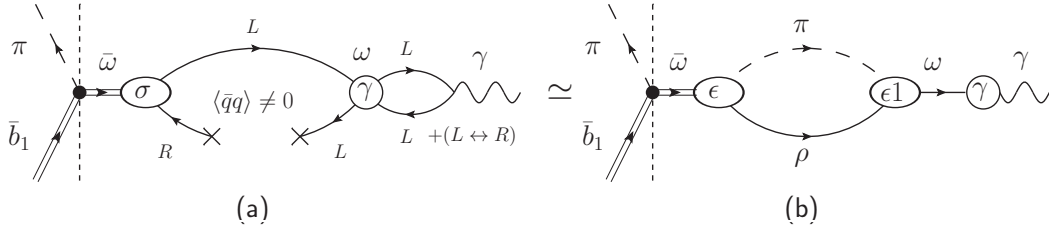


Figure 7. The decay of $\bar{b}_1 \rightarrow \pi\gamma$ through the $\omega(782)$ state, i.e., the VMD channel. (a) OPE description via QCD Lagrangian as inferred from Eq. (3.21) and (b) hadron interaction picture via anomalous coupling. In (a), the blobs with ‘ σ ’ and ‘ γ ’ represent the tensor and vector current representation, respectively, and the vertex ‘ ϵ ’ and ‘ $\epsilon 1$ ’ in (b) represent the anomalous hybrid state interpolation (4.20) and the physical interaction vertex (4.19), respectively.

the spin-1 mesonic states using the tensor representation for the purpose of searching for a VMD-evading process for the b_1 radiative decay. Because of the mixing of helicity states, the corresponding currents are not generally conserved in their parity or isospin eigenspace. If $SU(2)_{L,R}$ flavor symmetry is assumed, the four different spin-1 mesonic states reside in the grand $U(2)_L \otimes U(2)_R$ symmetry group [16].

As chiral symmetry is spontaneously broken, the \bar{b}_1 state in the tensor representation decays into the chiral partner $\bar{\omega}$ state by emitting a pion as the Goldstone boson. From the QCD sum rules analysis, we find that the \bar{b}_1 state can be identified as the physical $b_1(1235)$ state, while it is problematic to identify the $\bar{\omega}$ state as the physical $\omega(782)$ meson. The $\bar{\omega}$ state has the same spin and flavor quantum numbers as the $\omega(782)$ but it is found to have a much higher mass. Comparing the weighted OPE invariant with the anomalous loop-like spectral structure, the $\bar{\omega}$ state can be identified as the hybrid state of the π and ρ mesons. As there is no observed ω resonance state in the mass of around 1 GeV, the $\bar{\omega}$ state would be interpreted as an intermediate virtual state. It is well known that the vector current $J_\alpha^0 = \bar{q}T^0\gamma_\alpha q$ couples strongly to the vector meson state and the resulting spectral sum rules successfully reproduce the $\omega(782)$ mass [20–23]. Since the isoscalar component of $J_\alpha^{e.m.}$ is same as $(e_0/3)J_\alpha^0$, the nonzero invariant of Eq. (4.9) can be understood as the overlap between the $\bar{\omega}$ hybrid state and the physical $\omega(782)$ state, which then becomes the photon following the usual VMD scenario as depicted in Fig. 7 [6, 7].

However, the loop structure of the $\bar{\omega}$ state suggests other mechanisms of radiative decays of the b_1 . The π - ρ hybrid state can have an anomalous electromagnetic interaction as

$$\mathcal{L}_{\gamma\pi\rho}^{\epsilon 2} = \frac{e_0 g_{\gamma\pi\rho}}{2m_\rho} \epsilon^{\mu\bar{\mu}\alpha\bar{\alpha}} F_{\mu\bar{\mu}} \partial_\alpha \pi^a \rho_{\bar{\alpha}}^a \simeq \frac{e_0 g_{\gamma\pi\rho}}{m_\rho} F_{\mu\bar{\mu}} \bar{\omega}^{\mu\bar{\mu}}. \quad (5.1)$$

If the π and ρ are on-shell, the vertex can be substituted with Eq. (4.19) by the VMD hypothesis [10]. However, as most part of the loop phase space is off-shell, the direct photon coupling channel (5.1) can be distinguished from the VMD channel which could be the additional mechanism for the b_1 radiative decay as depicted in Fig. 8.

If the b_1 strongly couples to the tensor current, its decay is mediated mostly by the $\bar{\omega}$ state that is interpreted as the ρ - π hybrid state. Then the major decay process of the

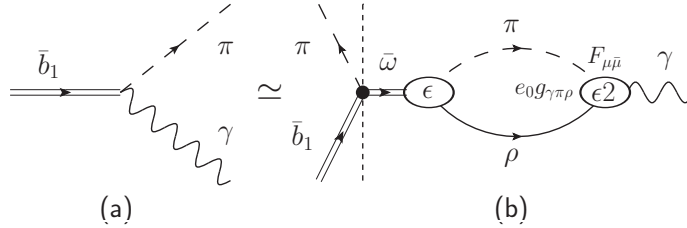


Figure 8. (a) The $\bar{b}_1 \rightarrow \pi\gamma$ decay not through the $\omega(782)$ state (direct channel) and (b) phenomenological description for the direct coupling between $\bar{\omega}$ and γ . The vertex ‘ ϵ ’ and ‘ $\epsilon'2$ ’ in (b) represent the anomalous hybrid state interpolation (4.20) and the physical interaction vertex given in Eq. (5.1), respectively.

b_1 meson would take the process of $b_1 \rightarrow \pi\bar{\omega} \rightarrow \pi\omega$, which involves the anomalous $\omega\rho\pi$ interaction. Because of the intermediate $\bar{\omega}$ state, the strong decay of the b_1 meson into two-pions, i.e., $b_1 \rightarrow \pi\pi\rho$, would be enhanced enough to be measured. However, because of the lack of experimental data, we cannot make a conclusion on the tensor representation of axial-vector mesons. For example, the direct decay of $b_1 \rightarrow \pi\pi\pi\pi$ was reported in 1960s [41], which concluded only that $\Gamma(b_1 \rightarrow \pi^+\pi^+\pi^-\pi^0, \text{direct})/\Gamma(b_1 \rightarrow \omega\pi) < 0.5$. More detailed information on the direct four-pion decays of the b_1 such as the precise value of the branching ratio and invariant mass distributions would be useful to understand the mechanisms of b_1 decay. Therefore, precise measurement of the details of the b_1 decay will shed light on our understanding on the structure and properties of axial-vector mesons and it can be performed at current experimental facilities.

A Tensor currents in $SU(2)_L \times SU(2)_R$ symmetry

A.1 Transformation of tensor currents in the non-relativistic limit

The quantum numbers of the mesonic state are defined at rest frame. Equations (3.1)-(3.4) show that each spin-1 state can be interpolated via tensor currents. Since the tensor current couples to both parity eigenstates, one can use dual tensor definition to describe a parity eigenstate in the opposite parity projection. For convenience, all the current is defined to interpolate spin-1 mesonic states in parity-odd projection. The infinitesimal $U_A(1)$ transformation on the \bar{b}_1 current reads

$$\begin{aligned}
 J_k^{\bar{b}_1, a} &= \frac{1}{2} \epsilon_{ijk} \bar{q} T^a \sigma_{ij} q \\
 &\rightarrow \frac{1}{2} \epsilon_{ijk} \bar{q} (I - i\alpha T^0 \gamma_5) T^a \sigma_{ij} (I - i\alpha T^0 \gamma_5) q + O(\alpha^2) \\
 &= \frac{1}{2} \epsilon_{ijk} \bar{q} T^a \sigma_{ij} q - i\alpha (-i\bar{q} T^a \sigma_{0k} q) + O(\alpha^2) \\
 &= J_k^{\bar{b}_1, a} - i\alpha (-iJ_k^{\rho, a}) + O(\alpha^2),
 \end{aligned} \tag{A.1}$$

where the corresponding commutation relations are summarized as

$$[Q_5^0, J_k^{\bar{b}_1, a}(x)] = -iJ_k^{\rho, a}(x), \quad [Q_5^0, J_k^{\rho, a}(x)] = iJ_k^{\bar{b}_1, a}(x). \tag{A.2}$$

Similarly, one can rotate quark fields via infinitesimal $SU(2)_L \times SU(2)_R$ rotation as

$$(1 - i\theta^b T^b) q_L \leftrightarrow q_L^\dagger (1 + i\theta^b T^b), \quad (\text{A.3})$$

$$(1 - i\delta^b T^b) q_R \leftrightarrow q_R^\dagger (1 + i\delta^b T^b). \quad (\text{A.4})$$

The transformation up to the leading order of θ^a and δ^a can be expressed in terms of explicit helicity states as

$$\begin{aligned} J_k^{\bar{b}_1, a} &= \frac{1}{2} \epsilon_{ijk} \bar{q} T^a \sigma_{ij} q = \bar{q}_L T^a \sigma_k q_R + \bar{q}_R T^a \sigma_k q_L \\ &\rightarrow \bar{q}_L T^a \sigma_k q_R + \bar{q}_R T^a \sigma_k q_L \\ &\quad + i\theta^b \left[\bar{q}_L \left(\frac{1}{4} \delta^{ab} \right) \sigma_k q_R + \bar{q}_L \left(\frac{i}{2} \epsilon^{bac} T^c \right) \sigma_k q_R \right. \\ &\quad \left. - \bar{q}_R \left(\frac{1}{4} \delta^{ab} \right) \sigma_k q_L - \bar{q}_R \left(\frac{i}{2} \epsilon^{abc} T^c \right) \sigma_k q_L \right] \\ &\quad - i\delta^b \left[\bar{q}_L \left(\frac{1}{4} \delta^{ab} \right) \sigma_k q_R + \bar{q}_L \left(\frac{i}{2} \epsilon^{abc} T^c \right) \sigma_k q_R \right. \\ &\quad \left. - \bar{q}_R \left(\frac{1}{4} \delta^{ab} \right) \sigma_k q_L - \bar{q}_R \left(\frac{i}{2} \epsilon^{bac} T^c \right) \sigma_k q_L \right] + O(\theta^2, \delta^2) \\ &\simeq \frac{1}{2} \epsilon_{ijk} \bar{q} T^a \sigma_{ij} q + \frac{i(\theta^b + \delta^b)}{2} \left(-i\epsilon^{abc} \frac{1}{2} \epsilon_{ijk} \bar{q} T^c \sigma_{ij} q \right) + \frac{i(\theta^a - \delta^a)}{2} (-i\bar{q} T^0 \sigma_{0k} q) \\ &= J_k^{\bar{b}_1, a} + \frac{i(\theta^b + \delta^b)}{2} \left(-i\epsilon^{abc} J_k^{\bar{b}_1, c} \right) + \frac{i(\theta^a - \delta^a)}{2} (-iJ_k^{\bar{\omega}}), \end{aligned} \quad (\text{A.5})$$

where the rotation directions ' $\theta^a = \delta^a$ ' and ' $\theta^a = -\delta^a$ ' correspond to $Q_v^a = \int d^3x q^\dagger(x) T^a q(x)$ and $Q_5^a = \int d^3x q^\dagger(x) T^a \gamma_5 q(x)$, respectively. The corresponding commutation relations read

$$[Q_5^a, J_k^{\bar{b}_1, b}(x)] = -i\delta^{ab} J_k^{\bar{\omega}}(x), \quad [Q_5^a, J_k^{\bar{\omega}}(x)] = iJ_k^{\bar{b}_1, a}(x), \quad [Q_v^a, J_k^{\bar{b}_1, b}(x)] = -i\epsilon^{abc} J_k^{\bar{b}_1, c}(x). \quad (\text{A.6})$$

Similar commutation relations can be obtained for other currents as

$$[Q_5^0, J_k^{\bar{\omega}}(x)] = -iJ_k^{\bar{h}_1}(x), \quad [Q_5^a, J_k^{\bar{\rho}, b}(x)] = i\delta^{ab} J_k^{\bar{h}_1}(x), \quad [Q_v^a, J_k^{\bar{\rho}, b}(x)] = -i\epsilon^{abc} J_k^{\bar{\rho}, c}(x). \quad (\text{A.7})$$

The mixing properties are diagrammatically described in Fig. 9.

A.2 Transformation of tensor currents in relativistic generalization

The covariant currents are defined as $J_{\mu\bar{\mu}}^0 \equiv \bar{q} T^0 \sigma_{\mu\bar{\mu}} q$ and $\tilde{J}_{\mu\bar{\mu}}^a \equiv -\frac{1}{2} \epsilon_{\mu\bar{\mu}\alpha\beta} \bar{q} T^a \sigma^{\alpha\beta} q$ to describe the $\bar{\omega}$ and \bar{b}_1 states, respectively, in the parity-odd projection at boosted frame.

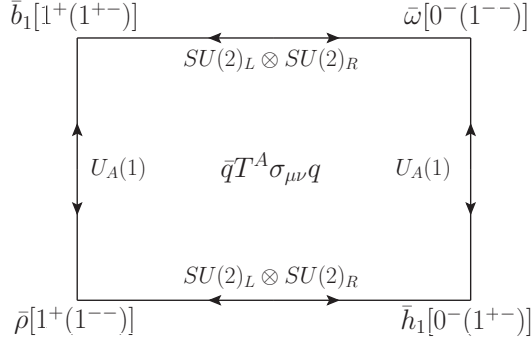


Figure 9. Four different spin-1 mesonic states in tensor representation under $U(1) \times SU(2)_L \times SU(2)_R$. These constitute quartet elements of $U(2)_L \times U(2)_R$.

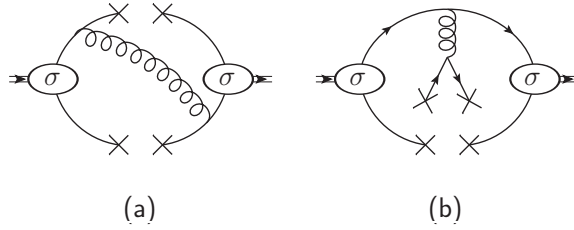


Figure 10. Diagrammatical description of the four-quark contributions in the OPE of correlator (4.2). (a) contribution to the invariant (4.6) and (b) the invariant (4.7). The blob with ‘ σ ’ represents the tensor current representation.

The flavor axial charge commutation relations are

$$\begin{aligned} [Q_5^a, J_{\mu\bar{\mu}}^0(x)] &\rightarrow -\bar{q}(x)T^a\gamma_5\sigma_{\mu\bar{\mu}}q(x) \\ &= -\frac{i}{2}\epsilon_{\mu\bar{\mu}\alpha\beta}\bar{q}(x)T^a\sigma^{\alpha\beta}q(x) = i\tilde{J}_{\mu\bar{\mu}}^a(x), \end{aligned} \quad (\text{A.8})$$

$$\begin{aligned} [Q_5^a, \tilde{J}_{\mu\bar{\mu}}^b(x)] &\rightarrow \frac{1}{2}\epsilon_{\mu\bar{\mu}\alpha\beta}\delta^{ab}\bar{q}(x)T^0\gamma_5\sigma^{\alpha\beta}q(x) \\ &= \frac{1}{2}\epsilon_{\mu\bar{\mu}\alpha\beta}\frac{i}{2}\epsilon^{\alpha\beta\nu\bar{\nu}}\delta^{ab}\bar{q}(x)T^0\sigma_{\nu\bar{\nu}}q(x) = -i\delta^{ab}J_{\mu\bar{\mu}}^0(x). \end{aligned} \quad (\text{A.9})$$

Similarly, the other commutation relations can be obtained in covariant generalization as

$$[Q_5^a, J_{\mu\bar{\mu}}^b(x)] = -i\delta^{ab}\tilde{J}_{\mu\bar{\mu}}^0(x), \quad [Q_5^a, \tilde{J}_{\mu\bar{\mu}}^0(x)] = iJ_{\mu\bar{\mu}}^a(x), \quad (\text{A.10})$$

$$[Q_5^0, \tilde{J}_{\mu\bar{\mu}}^a(x)] = -iJ_{\mu\bar{\mu}}^a(x), \quad [Q_5^0, J_{\mu\bar{\mu}}^a(x)] = i\tilde{J}_{\mu\bar{\mu}}^a(x), \quad (\text{A.11})$$

$$[Q_5^0, J_{\mu\bar{\mu}}^0(x)] = -i\tilde{J}_{\mu\bar{\mu}}^0(x), \quad [Q_5^0, \tilde{J}_{\mu\bar{\mu}}^0(x)] = iJ_{\mu\bar{\mu}}^0(x). \quad (\text{A.12})$$

These lead to the same diagrammatical summarization presented in Fig. 9.

B Technical remarks on sum rules analysis

B.1 Four-quark condensates

In the OPE of the tensor current correlator, the four-quark condensate terms are the lowest mass-dimensional quark contribution. These condensates determine the asymptotic behav-

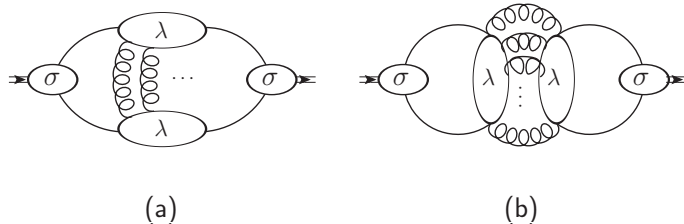


Figure 11. Correlation types of the mesonic quantum numbers: (a) connected and (b) disconnected correlation of Dirac eigenmodes. Here, ‘ σ ’ in the blob and ‘ λ ’ in the quark correlation represent the tensor current representation and the Dirac eigenmode, respectively.

ior of the Borel curves and distinguish parity eigenstates. The condensates in Eqs. (4.14) and (4.15) give huge contribution to the sum rules because the Wilson coefficient of the invariant term of Eq. (4.6) is dominant over the others. The corresponding diagrammatical description can be found in Fig. 10(a). Unfortunately, the values of these four-quark condensates are unknown at present, and are thus estimated, for example, by adopting the vacuum saturation hypothesis. However, the usual factorization scheme does not reflect all the possible contributions in the condensates. In the condensates defined in Eqs. (4.14) and (4.15), isospin and color matrices appear in the condensates, and the usual factorization scheme only allows ‘quark connected’ correlations as in Fig. 11(a) when there are isospin matrices in the quark bilinears. Although isovector terms cannot have ‘quark disconnected’ contribution [Fig. 11(b)], the isoscalar terms can have contributions even if they are colored. One can consider the non-local generalization of meson interpolating current,

$$M_{\mu\bar{\mu}}^A(y, x; c) = \bar{q}(y)T^A\sigma_{\mu\bar{\mu}} \exp \left[ig \int_x^y dz^\nu A_\nu(z) \right] q(x). \quad (\text{B.1})$$

Then, in the very small but nonzero space-time separation $\epsilon = |y - x| \neq 0 \ll 1$ which can be allowed in the relevant hadron size for the quark correlation average, gauge corrections are needed to fix the initial and final interpolated states on the equivalent gauge orbit [Fig. 11(b)]. Therefore, if the pair of colored isoscalar bilinear appears in totally color blind configuration, there is no reason to discard disconnected contribution. Considering that the relative sign between two contributions is negative, the magnitude of the isoscalar parameter is assigned to be smaller than that of the isovector parameter: $|\alpha_0| < |\alpha_a|$, $|\beta_0| < |\beta_a|$.

We now consider the condensates containing pseudoscalar type bilinear as in Eq. (4.15). Since ψ_0 and $\gamma_5\psi_0$ reside in the same eigenspace ($\lambda = 0$), the vacuum average of pseudoscalar bilinear does not vanish in the nontrivial gauge configuration [40]:

$$\langle \bar{q}\gamma_5 q \rangle_\nu = - \lim_{m_q \rightarrow 0} \left\langle \sum_\lambda \frac{\psi_\lambda^\dagger \gamma_5 \psi_\lambda}{m_q - i\lambda} \right\rangle = -\pi(n_R - n_L) \equiv \pi\nu, \quad (\text{B.2})$$

where ν denotes the winding number, and the inner product between the modes in different eigenspace vanishes. If all the gauge configuration is summed up, the vacuum average can

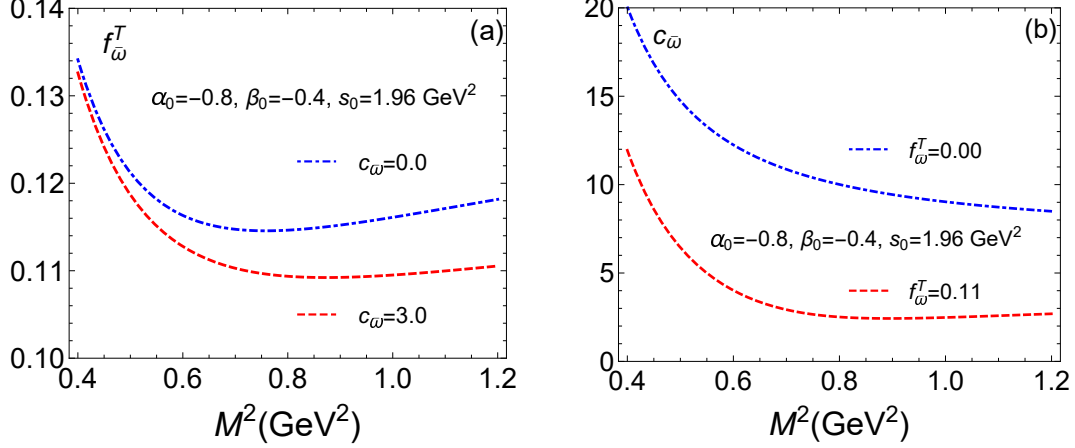


Figure 12. Borel curve (a) for the meson pole residue $f_{\bar{\omega}}^T$ and (b) for the tensor current-hybrid coupling $c_{\bar{\omega}}^{\text{hy}}$ with reversed parameter set ($\alpha_0 = -0.8$, $\beta_0 = -0.4$).

be written as

$$\langle \bar{q}\gamma_5 q \rangle = \sum_{\nu} e^{i\nu\theta} \langle \bar{q}\gamma_5 q \rangle_{\nu} = 2\pi i \sum_{\nu=0}^{\infty} \nu \sin \nu\theta \simeq 0, \quad (\text{B.3})$$

where θ is the QCD vacuum angle. However, for the quark correlation in the four-quark vacuum average, the nontrivial topological contribution should appear in terms of ν^2 and would not vanish in the summation. In this study, the nontrivial contribution is assumed to appear as an alternating series of ν^2 in Eq. (4.15) while it does not in Eq. (4.14), which leads to $|\alpha_A| > |\beta_A|$.

The condensate (4.16) contributes to the invariant piece (4.7) whose diagrammatical description is given in Fig. 10(b). As the vector bilinear is obtained from the field equation of the gluons, at least the sign of the usual factorization estimation has been justified in Euclidean space [20]. Therefore we take the usual vacuum saturation value of $\gamma = 1$. Furthermore, its contribution in Eq. (4.7) is much smaller than those from the other four-quark condensates so that a slightly different value for gamma will not change the main result of the present work.

B.2 Supplementary remarks for the sum rules with $\alpha_A < 0$, $\beta_A < 0$

In the previous arguments, the proper sets ($\alpha_0 = 0.8$, $\beta_0 = 0.4$) and ($\alpha_a = 1.0$, $\beta_a = 0.5$) have been used for Borel sum rules for the $\bar{\omega}$ and \bar{b}_1 states, respectively. If we use the reversed sign of the parameter set, the Borel curves for $f_{\bar{\omega}}^T$ and $c_{\bar{\omega}}^{\text{hy}}$ are obtained as shown in Fig. 12 and Fig. 13, respectively. In this case, $f_{\bar{\omega}}^T$ shows plateau-like behavior even in the one-particle pole limit ($c_{\bar{\omega}}^{\text{hy}} = 0$). In the optimized condition, the stable Borel curves provide $f_{\bar{\omega}}^T = 0.11$ and $c_{\bar{\omega}}^{\text{hy}} = 2.0$ as plateau values. It is found that the magnitude of $f_{\bar{\omega}}^T$ reduces to 90% when we vary $c_{\bar{\omega}}^{\text{hy}}$ from 0 to 2.0, while $c_{\bar{\omega}}^{\text{hy}}$ becomes 20% of its original value when we change $f_{\bar{\omega}}^T$ from 0 to 0.11. This means that the $\bar{\omega}$ state becomes dominated by the one-particle mesonic state with the set of ($\alpha_0 = -0.8$, $\beta_0 = -0.4$).

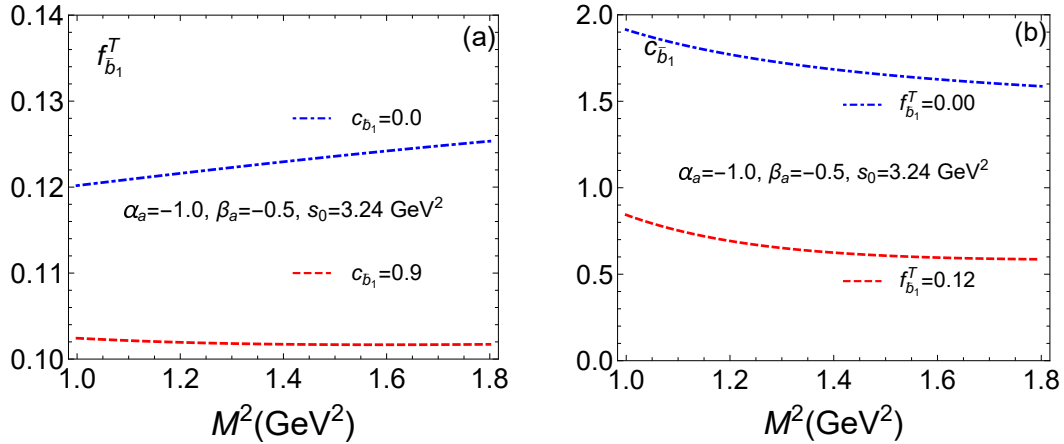


Figure 13. Borel curve (a) for the meson pole residue $f_{b_1}^T$ and (b) for the tensor current-hybrid coupling $c_{b_1}^{\text{hy}}$ with reversed parameter set ($\alpha_a = -1.0$, $\beta_a = -0.5$).

However, this tendency becomes unclear in the case of the \bar{b}_1 analysis. As one can find in Fig. 13, $f_{b_1}^T$ and $c_{b_1}^{\text{hy}}$ do not show stable behavior with $c_{b_1}^{\text{hy}} = 0$ and $f_{b_1}^T = 0.00$, respectively. In the optimized condition, even though the Borel curve for $f_{b_1}^T$ strongly depends on the continuum threshold, the scale of each coupling strength becomes about 80% and 45% of their original magnitudes when we vary $c_{b_1}^{\text{hy}}$ from 0 to 0.9 and $f_{b_1}^T$ from 0 to 0.12, respectively. This observation then leads us to the conclusion that the \bar{b}_1 state is dominated by the one-particle meson state within the set of ($\alpha_a = -1.0$, $\beta_a = -0.5$). This result leads to the usual VMD scenario ($b_1 \rightarrow \pi\omega \rightarrow \pi\gamma$).

Considering that the Borel curve for $f_{b_1}^T$ is highly dependent of the parameter set, it is possible that the non-negligible part of \bar{b}_1 could be a π - ω hybrid state. However, this kind of hybrid state leads to a stable $\omega(782)$ state after pion breaking, where the VMD scenario for the radiative decay is still valid.

B.3 Borel sum rules

By assuming regularity of the correlation function, the invariants can be written in dispersion relation as

$$\Pi_i(q^2) = \frac{1}{2\pi i} \int_0^\infty ds \frac{\Delta\Pi_i(s)}{s - q^2} + P_n(q^2), \quad (\text{B.4})$$

where $P_n(q^2)$ is the finite order polynomial in q^2 , which comes from the integration on the circle of contour on complex plane and the discontinuity $\Delta\Pi_i(s) \equiv \lim_{\epsilon \rightarrow 0^+} [\Pi_i(s + i\epsilon) - \Pi_i(s - i\epsilon)] = 2i \text{Im}[\Pi_i(s + i\epsilon)]$ is defined on the positive real axis. Then all the possible physical states are contained in this discontinuity. In the phenomenological point of view, the invariant can be assumed to have a pole and continuum structure as

$$\Delta\Pi_i(s) = \Delta\Pi_i^{\text{pole}}(s) + \theta(s - s_0)\Delta\Pi_i^{\text{OPE}}(s), \quad (\text{B.5})$$

where s_0 represents the continuum threshold. To suppress the continuum contribution, the weight function $W(s) = e^{-s/M^2}$ may be used as

$$\mathcal{W}_M[\Pi_i(q^2)] = \frac{1}{2\pi i} \int_0^\infty ds e^{-s/M^2} \Delta\Pi_i(s). \quad (\text{B.6})$$

The corresponding differential operator \mathcal{B} can be defined as

$$\mathcal{B}[f(-q^2)] \equiv \lim_{\substack{-q^2, n \rightarrow \infty \\ -q^2/n = M^2}} \frac{(-q^2)^{n+1}}{n!} \left(\frac{\partial}{\partial q^2} \right)^n f(-q^2). \quad (\text{B.7})$$

By making use of this operator in Eq. (B.4), one obtains

$$\mathcal{W}_M[\Pi_i(q^2)] = \frac{1}{2\pi i} \int_0^\infty ds e^{-s/M^2} \Delta\Pi_i(s) = \mathcal{B}[\Pi_i(q^2)], \quad (\text{B.8})$$

where following relation has been used:

$$\mathcal{B} \left[\frac{1}{s - q^2} \right] = e^{-s/M^2}. \quad (\text{B.9})$$

The residues located after the continuum threshold with finite s_0 can be subtracted as

$$\mathcal{W}_M^{\text{subt.}}[\Pi_i(q^2)] = \frac{1}{2\pi i} \int_0^{s_0} ds e^{-s/M^2} \Delta\Pi_i(s) = \mathcal{B}[\Pi_i(q^2)]_{\text{subt.}}. \quad (\text{B.10})$$

Using the following integral identities,

$$\int_{s_0}^\infty ds e^{-s/M^2} = M^2 e^{-s_0/M^2}, \quad (\text{B.11})$$

$$\int_{s_0}^\infty ds s e^{-s/M^2} = (M^2)^2 e^{-s_0/M^2} (s_0/M^2 + 1), \quad (\text{B.12})$$

$$\int_{s_0}^\infty ds s^2 e^{-s/M^2} = (M^2)^3 e^{-s_0/M^2} (s_0^2/2M^4 + s_0/M^2 + 1), \quad (\text{B.13})$$

the subtraction of continuum contribution for the OPE side can be summarized as

$$E_0(s_0) \equiv 1 - e^{-s_0/M^2}, \quad (\text{B.14})$$

$$E_1(s_0) \equiv 1 - e^{-s_0/M^2} (s_0/M^2 + 1), \quad (\text{B.15})$$

$$E_2(s_0) \equiv 1 - e^{-s_0/M^2} (s_0^2/2M^4 + s_0/M^2 + 1). \quad (\text{B.16})$$

These results are used when E_n is multiplied to all $(M^2)^{n+1}$ terms in $\mathcal{B}[\Pi_i(q^2)]$. This weighting scheme and subsequent spectral sum rules are known as the Borel transformation and Borel sum rules, respectively.

Acknowledgments

This work was supported by the National Research Foundation of Korea under Grant Nos. NRF-2017R1D1A1B03033685 (K.S.J.), NRF-2016R1D1A1B03930089 (S.H.L.), and NRF-2015R1D1A1A01059603 (Y.O.).

References

- [1] **Particle Data Group**, C. Patrignani et al., *Review of particle physics*, *Chin. Phys. C* **40** (2016) 100001.
- [2] **Brookhaven E852 Collaboration**, M. Nozar, et al., *A study of the reaction $\pi^- p \rightarrow \omega \pi^- p$ at 18 GeV/c: the D and S decay amplitudes for $b_1(1235) \rightarrow \omega \pi$* , *Phys. Lett. B* **541** (2002) 35.
- [3] B. Collick, S. Heppelmann, T. Joyce, Y. Makdisi, et al., *Primakoff production of the $B^+(1235)$ meson*, *Phys. Rev. Lett.* **53** (1984) 2374.
- [4] T. D. Lee, S. Weinberg, and B. Zumino, *Algebra of fields*, *Phys. Rev. Lett.* **18** (1967) 1029.
- [5] N. M. Kroll, T. D. Lee, and B. Zumino, *Neutral vector mesons and the hadronic electromagnetic current*, *Phys. Rev.* **157** (1967) 1376.
- [6] G. J. Gounaris and J. J. Sakurai, *Finite-width corrections to the vector-meson-dominance prediction for $\rho \rightarrow e^+ e^-$* , *Phys. Rev. Lett.* **21** (1968) 244.
- [7] J. J. Sakurai and D. Schildknecht, *Generalized vector dominance and inelastic electron-proton scattering*, *Phys. Lett.* **40B** (1972) 121.
- [8] R. P. Feynman, *Photon-Hadron Interactions*. W. A. Benjamin, Reading, MA, 1972.
- [9] I. Zahed and G. E. Brown, *The Skyrme model*, *Phys. Rep.* **142** (1986) 1.
- [10] U.-G. Meissner, *Low-energy hadron physics from effective chiral Lagrangians with vector mesons*, *Phys. Rep.* **161** (1988) 213.
- [11] T. Fujiwara, T. Kugo, H. Terao, S. Uehara, and K. Yamawaki, *Non-abelian anomaly and vector mesons as dynamical gauge bosons of hidden local symmetries*, *Prog. Theor. Phys* **73** (1985) 926.
- [12] M. Bando, T. Kugo, and K. Yamawaki, *Nonlinear realization and hidden local symmetries*, *Phys. Rep.* **164** (1988) 217.
- [13] J. L. Rosner, *Decays of $l = 1$ mesons to $\gamma \pi$, $\gamma \rho$, and $\gamma \gamma$* , *Phys. Rev. D* **23** (1981) 1127.
- [14] S. Ishida, K. Yamada, and M. Oda, *Radiative decays of light-quark S- and P-wave mesons in the covariant oscillator quark model*, *Phys. Rev. D* **40** (1989) 1497.
- [15] V. L. Chernyak and A. R. Zhitnitsky, *Asymptotic behaviour of exclusive processes in QCD*, *Phys. Rep.* **112** (1984) 173.
- [16] T. Cohen and X. Ji, *Chiral multiplets of hadron currents*, *Phys. Rev. D* **55** (1997) 6870.
- [17] K. G. Wilson and W. Zimmermann, *Operator product expansions and composite field operators in the general framework of quantum field theory*, *Commun. Math. Phys.* **24** (1972) 87.
- [18] M. Gell-Mann, *Symmetries of baryons and mesons*, *Phys. Rev.* **125** (1962) 1067.
- [19] M. Gell-Mann, R. J. Oakes, and B. Renner, *Behavior of current divergences under $SU_3 \times SU_3$* , *Phys. Rev.* **175** (1968) 2195.
- [20] M. A. Shifman, A. I. Vainshtein, and V. I. Zakharov, *QCD and resonance physics. Theoretical foundations*, *Nucl. Phys. B* **147** (1979) 385.
- [21] M. A. Shifman, A. I. Vainshtein, and V. I. Zakharov, *QCD and resonance physics. Applications*, *Nucl. Phys. B* **147** (1979) 448.

- [22] M. A. Shifman, A. I. Vainshtein, and V. I. Zakharov, *QCD and resonance physics. The ρ - ω mixing*, *Nucl. Phys. B* **147** (1979) 519.
- [23] L. J. Reinders, H. Rubinstein, and S. Yazaki, *Hadron properties from QCD sum rules*, *Phys. Rep.* **127** (1985) 1.
- [24] J. Govaerts, L. J. Reinders, F. de Viron, and J. Weyers, *$l = 1$ mesons and the four-quark condensate in QCD sum rules*, *Nucl. Phys. B* **283** (1987) 706.
- [25] P. Ball and V. M. Braun, *ρ meson light-cone distribution amplitudes of leading twist reexamined*, *Phys. Rev. D* **54** (1996) 2182.
- [26] N. S. Craigie and H. Dorn, *On the renormalization and short-distance properties of hadronic operators in QCD*, *Nucl. Phys. B* **185** (1981) 204.
- [27] T. Banks and A. Casher, *Chiral symmetry breaking in confining theories*, *Nucl. Phys. B* **169** (1980) 103.
- [28] H. Leutwyler and A. Smilga, *Spectrum of Dirac operator and role of winding number in QCD*, *Phys. Rev. D* **46** (1992) 5607.
- [29] N. Evans, S. D. H. Hsu, and M. Schwetz, *Topological charge and $U(1)_A$ symmetry in the high temperature phase of QCD*, *Phys. Lett. B* **375** (1996) 262.
- [30] T. D. Cohen, *QCD inequalities, the high temperature phase of QCD, and $U(1)_A$ symmetry*, *Phys. Rev. D* **54** (1996) R1867.
- [31] S. H. Lee and T. Hatsuda, *$U_A(1)$ symmetry restoration in QCD with N_f flavors*, *Phys. Rev. D* **54** (1996) R1871.
- [32] S. H. Lee and S. Cho, *Chiral and $U_A(1)$ symmetry in correlation functions in medium*, *Int. J. Mod. Phys. E* **22** (2013) 1330008.
- [33] N. Isgur, C. Morningstar, and C. Reader, *The a_1 in τ decay*, *Phys. Rev. D* **39** (1989) 1357.
- [34] Y. Oh and T.-S. H. Lee, *One-loop corrections to ω photoproduction near threshold*, *Phys. Rev. C* **66** (2002) 045201.
- [35] M. Barmawi, *Regge-pole contribution to vector-meson production*, *Phys. Rev.* **142** (1966) 1088.
- [36] M. Barmawi, *Regge-pole analysis of $\pi^+ + n \rightarrow \omega + p$* , *Phys. Rev. Lett.* **16** (1966) 595.
- [37] M. Barmawi, *Application of a Regge-pole model to the reactions $\pi^- p \rightarrow \pi^0 n$, $\pi^- p \rightarrow \eta n$, and $\pi^+ n \rightarrow \omega p$* , *Phys. Rev.* **166** (1968) 1857.
- [38] J. Wess and B. Zumino, *Consequences of anomalous Ward identities*, *Phys. Lett.* **37B** (1971) 95.
- [39] O. Kaymakcalan, S. Rajeev, and J. Schechter, *Non-abelian anomaly and vector-meson decays*, *Phys. Rev. D* **30** (1984) 594.
- [40] S. Coleman, *Aspects of Symmetry*. Cambridge Univ. Press, Cambridge, 1985.
- [41] M. Abolins, R. L. Jander, W. A. W. Mehlop, N. h. Xuong, P. M. Yager, *Production of multimeson resonances by $\pi^+ p$ interaction and evidence for a $\pi\omega$ resonance vector-meson decays*, *Phys. Rev. Lett.* **11** (1963) 381.